Gating System Design Optimization for Sand Casting

M.Tech Dissertation

Submitted in partial fulfillment of the requirements for the award of degree of

Master of Technology
(Manufacturing Engineering)

by

Dolar Vaghasia

(07310032)

Supervisor

Prof. B. Ravi

Department of Mechanical Engineering
Indian Institute of Technology Bombay
June 2009

Declaration of Academic Integrity

I declare that this written submission represents my ideas in my own words and where others' ideas or words have been included, I have adequately cited and referenced the original sources. I also declare that I have adhered to all principles of academic honesty and integrity and have not misrepresented or fabricated or falsified any idea/data/fact/source in my submission. I understand that any violation of the above will be cause for disciplinary action as per the rules of regulations of the Institute.

Vaghasia Dolar Kanjibhai

ABSTRACT

Many products are made using casting process as it is economical and has the ability to produce intricate shapes. Casting software can optimize the virtual castings so that real castings can be produced ‘right first time and every time’. This however, requires a well designed methodology for gating system optimization.

For sound casting, we need to optimize the gating system for a given geometry of casting. The literature available on gating design optimization recommends maximizing yield, minimizing ingate velocity of molten metal, optimizing the ingate location and minimizing the warpage. There is no reported work based on maximizing the filling rate of molten metal in the casting cavity. Maximum filling rate is critical in thin and long castings which lose heat vary rapidly, and higher filling rate helps to avoid defects like cold shut and misrun. It is also useful wherein it is required to increase the production rate of casting.

A systematic methodology for gating design optimization considering filling rate maximization has been developed based on limiting constraints. These include pouring time, modulus of ingate, mold erosion, Reynolds number at ingate section and filling rate of molten metal. The various steps to achieve the optimized gating dimensions include specifying the attribute values as input for the process, calculation of constraints, optimization process and computing gating dimensions.

The constraint equations are formulated in the form of design variables that is, ingate area and velocity of molten metal at ingate. For optimization process, a Sequential Quadratic Programming (SQP) technique is used, The SQP algorithm is implemented by coding in Matlab. A case study is presented using the proposed methodology for finding the optimized gating dimensions.

Table of Contents

List of Figures

NOMENCLATURE

A	Total cooling surface area of the casting
A_g	Cross sectional area of ingate
A_i	Instantaneous cross sectional area of casting layer being filled
$A_s : A_r : A_g$	Gating ratio
d	Characteristic length of the flow through the ingate section
dl	Layer thickness
F_T	Tangential force exerted by the melt-jet
F_N	Normal force exerted by the melt-jet
f	Permeability of sand
g	Acceleration due to gravity
h	Instantaneous height of molten metal in the mold cavity
h_m	Mold cavity height
h_t	Height between bottom of mold cavity to the top of the mold
h^*	Vertical height between parting plane and mold bottom plane
K_{mold}	Thermal conductivity of the mold
M_{conne_sec}	Modulus of the section connected to ingate
M_{ingate}	Modulus of ingate
$m_{air}(i)$	Mass of air present in the mold cavity at any time instant τ_i
$\dot{m}$	Initial mass flow rate of molten metal in the mold cavity
P_{CO_2}	Partial pressure exerted by the CO_2 gas in a gas mixture
P_{H_2}	Partial pressure exerted by the H_2 gas in a gas mixture
P_{N_2}	Partial pressure exerted by the N_2 gas in a gas mixture
P_{O_2}	Partial pressure exerted by the O_2 gas in a gas mixture
$P_{air}(i)$	Partial pressure exerted by the air on the molten metal at time instant τ_i
P_g	Wetted perimeter of the ingate section
$P_{gas\_per\_i}$	Pressure drop due to permeability of sand at time instant τ_i
$P_{metallostatic}$	Pressure exerted by molten metal due to metallostatic head

P_{mold_i}	Total pressure of the generated gases and air in the cavity at time instant i
Q	Initial volume flow rate of molten metal
R_{CO_2}	Gas constant for CO_2 gas
R_{H_2}	Gas constant for H_2 gas
R_{H_2O}	Gas constant for water
R_{N_2}	Gas constant for N_2 gas
R_{O_2}	Gas constant for O_2 gas
R_e	Reynolds Number
S_S	Mold shear strength
S_Y	Mold compressive strength
T_m	Melting point temperature of metal
T_p	Pouring temperature of molten metal
t_{eff}	Effective thickness
t_{flight}	Time taken by the melt-jet from ingate to the mold bottom surface
t_{mold}	Thickness of mold
V	Volume of casting
$V(i)$	Volume of gases at any time instant τ_i
V_H	Horizontal component of melt-jet velocity
V_{Layer_i}	Volume of metal layer at any time instant τ_i
V_Y	Vertical component of melt-jet velocity
$V_{impinge}$	Resultant impingement velocity of melt-jet at the mold bottom surface
V_g	Velocity of molten metal at ingate
V_{sand}	Total volume of molding sand

Greek characters

γ_m	Kinematic viscosity of the molten metal
η_{CO_2}	No. of moles of CO_2 present in the mold cavity
η_{H_2}	No. of moles of H_2 present in the mold cavity
η_{N_2}	No. of moles of N_2 present in the mold cavity
η_{O_2}	No. of moles of O_2 present in the mold cavity
μ_m	Dynamic viscosity of the molten metal
θ	Angle made by melt jet with a horizontal plane at any time instant
ρ_{H_2O}	Density of water
ρ_m	Density of molten metal
$\rho_{sea-coal}$	Density of sea coal
σ_S	Shear stress induced in the mold bottom surface
σ_Y	Compressive stress induced in the mold bottom surface
τ_f	Pouring time or filling time of mold cavity
τ_f^*	Time elapsed between pouring temperature to start of solidification temp.
τ_i	Time taken by molten metal to fill up to i^{th} layer

Chapter 1

Introduction

In casting process, gating system plays an important role to produce a high quality casting. A poorly designed gating system results in casting defects. A gating system controls mould filling process. The main function of gating system is to lead clean molten metal from ladle to the casting cavity ensuring smooth, uniform and complete filling. Hence to design a good gating system one must know the behavior of fluid flow during mould filling process. Mould filling is a complex phenomenon, influencing both internal and external quality. The flow of molten metal after being poured is a transient phenomena accompanied by turbulence, separation of the flow from the boundaries, dividing and combined flow at the junction, simultaneous heat transfer during the flow and onset of solidification. Moreover melt properties like density, viscosity and surface tension are continuously changing during the flow. All this together makes the filling analysis quite complex.

An optimized gating design satisfying this entire requirement is obtained by experimentation through trial and error methods for a given casting geometry. However, this method takes a long time to get the optimal dimensions of the gating channels and also adds cost to the company. Another approach is to form the mathematical model that represents the actual mould filling process, so that we can predict the results in advance before producing actual casting. This mathematical model is then implemented in a suitable optimization algorithm which optimizes the process parameters along with satisfying all the process constraints. Hence physical experiment is replaced by numerical experiment by this method. This process saves time by applying an accurate and precise numerical optimization technique. Research work published on optimization of gating system recommends maximizing the yield, minimizing the ingate velocity of molten metal, optimizing the ingate location and minimizing warpage. However, no one appears to have focused on maximizing the filling rate of molten metal.

So to produce a casting that is free from the pouring related defects and has optimal gating dimensions based on filling rate, there is a need to develop a methodology that optimizes the gating dimensions considering the constraints of pouring related defects.

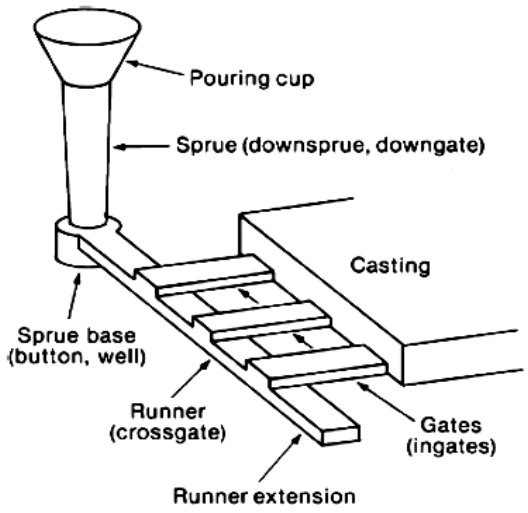

Figure 1.1 Basic elements of gating system

1.1 Basic Elements of Gating System

The elements of gating system includes pouring basin, sprue, sprue well, runner and ingate, in the sequence of flow of molten metal from ladle to the mould cavity as shown in figure 1.1.

Pouring Basin

It is the funnel-shaped opening, made at the top of the mold. The main purpose of the pouring basin is to direct the flow of molten metal from ladle to the sprue. It should be made substantially large and is kept near the edge of the mold box. Pouring basin must be deep enough to reduce the vortex formation and is kept full during entire pouring operation.

Sprue

It is a passage which connects the pouring basin to the runner or ingate. It is generally made tapered downward to avoid aspiration of air. The cross section of the sprue may be square, rectangular, or circular. The round sprue has a minimal surface area exposed to cooling and offers the lowest resistance to the flow of metal. The square or rectangular sprue minimizes the air aspiration and turbulence.

Sprue well

It is located at the base of the sprue. It arrests the free fall of molten metal through the sprue and turns it by a right angle towards the runner.

Cross-gate or Runner

In case of large casting, the fluidity length of the molten metal is less than the maximum distance required to be travelled by the molten metal along the flow path. So it is necessary to provide the multiple ingates to reduce the maximum flow distance needed to be travelled by the molten metal. Moreover, in a multi-cavity mould also each cavity must have at least one ingate, therefore it is necessary to connect all the ingate to a common passage-way which is finally linked with the sprue to complete the flow path. This passage way is called runner. The cross section of the runner is usually rectangular to get a streamlined flow with less turbulence. The runner must fill completely before letting the molten metal enter the ingates. In castings where more than one ingate is present, the cross sectional area must be reduced after each ingate (by an amount equal to area of that ingate), to ensure the uniform flow through the ingates.

Ingate or Gate

It is a small passage which connects the runner to the mould cavity. The cross section is square, rectangular and trapezoidal.

1.2 Gating System and Types

a) Depending upon the orientation of the parting plane, the gating system can be classified as horizontal and vertical gating systems as shown in figure 1.2.

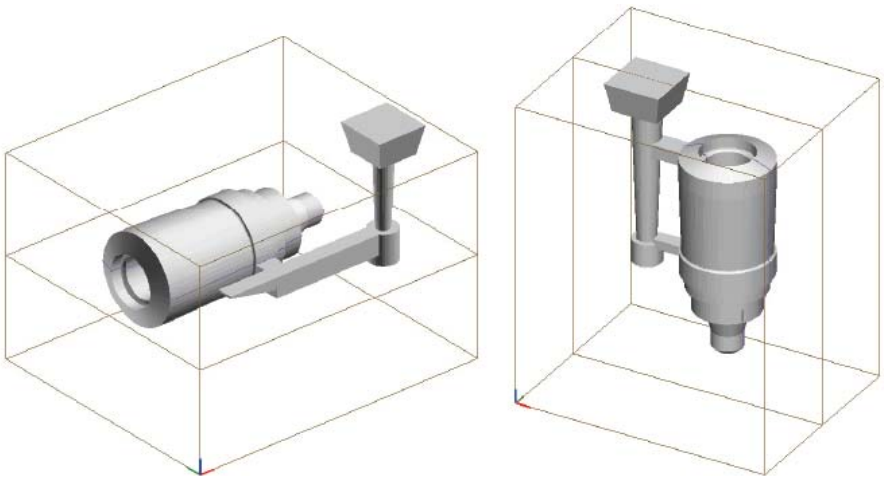

(a) Horizontal gating system (b) Vertical gating system

Figure 1.2 Classification of gating system based on parting plane orientation

Horizontal Gating System

In horizontal gating systems, parting plane is horizontal and contains runners and ingates. The sprue is vertical, perpendicular to the parting plane. These are suitable for flat castings filled under gravity, such as in green sand casting and gravity die casting.

Vertical Gating System

In the vertical gating system, parting plane is vertical and contains runners and ingates. For gravity filling processes (high pressure sand molding, shell molding and gravity die casting) the sprue is vertical and for pressure die casting sprue is along the parting plane. It is suitable for tall castings.

b) Depending upon the position of ingate(s), horizontal gating systems can be classified as top, bottom and parting line gating system as shown in figure 1.3.

Top Gating System

In top gating molten metal from the pouring basin flows to the mold cavity directly from the top of the mold cavity. The advantage of the top gating is that it promotes directional solidification from bottom to the top of the casting cavity. The disadvantage is that the free fall of the hot molten metal causes mold erosion. It is suitable only for flat casting. The velocity of molten metal remains constants at the ingate from start to the end of filling, so top gating gives fastest filling rate as compared to the bottom and parting line gate.

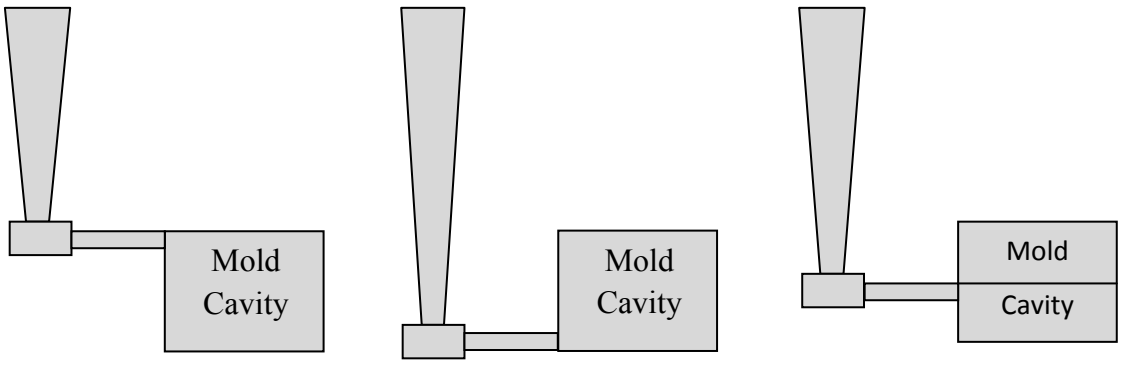

(a) Top gating (b) Bottom gating (c) Parting line gating

Figure 1.3 Classification of gating system based on position of ingates

Bottom Gating System

In bottom gating molten metal enters from the bottom of the casting cavity. It is recommended for tall casting where free fall of molten metal has to be avoided. The advantage of the bottom gating is that molten metal enters the bottom of the cavity gradually with minimal disturbances. The only disadvantage is that casting cavity is filled with variable filling rate, having high velocity of molten metal at the start of filling and gradually decreasing velocity as the molten metal fills the cavity.

Parting-line Gating System

In a parting-line gating system the gating channel are located at the parting plane, usually at the middle. It combines the advantages of both top and bottom gating system by reducing the free fall height of the metal to almost half of the mold height and allowing high filling rate as compared to the bottom gating system. Turbulence effect is also minimized as compared to top gating system. The most commonly used gating system is horizontal gating system with ingates at the parting plane.

c) Depending on the ratio of total cross sectional area of sprue exit, runner and ingate $\left(A_s : A_r : A_g\right)$, gating system is divided into pressurized system and non pressurized system.

Pressurized System

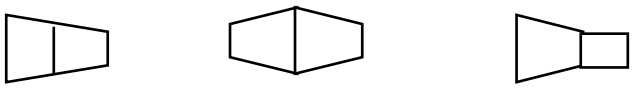

1:0.75:0.5 1:2:0.75 2:1:1

In this system pressure is maintained at the ingates by the fluid. In order to achieve this total gate area should be less than the sprue exit area $\left(A_g < A_s\right)$. In other words choke is located at the ingate. This system keeps gating channels full of metal. Due to pressurization the flow separation is absent in the system also air aspiration is minimized. The filling rate and yield increase. However, high metal velocity will cause turbulence.

Non Pressurized System

In this system choke is located at the sprue exit. Hence the sprue exit area is less than the total gate area $\left(A_s < A_g \right)$, for example 1:2:2, 1:4:4. Due to lower velocity, filling rate will be less. The process yield increases but it suffers from the disadvantage of flow separation.

1.3 Filling related Defects

There are three types of casting defects related to filling : incomplete filling, solid inclusion and gaseous entrapments.

Incomplete Filling

It is caused by poor fluidity of molten metal and results in cold shut or misrun. Cold shut occurs when two streams of molten metal coming from the opposite directions meet, but do not fuse together completely. A misrun occurs when the hot molten metal does not fill thin or end section completely.

Solid Inclusion

It is caused by high turbulence of molten metal during filling and results in the form of sand inclusion and slag inclusion. Sand inclusion occurs due to bulk turbulence in the gating channels resulting in the erosion of sand from the mold walls. Slag inclusions are caused by surface turbulence along the path of molten metal.

Gaseous Entrapments

Gaseous or air entrapment appears in the form of blow hole or gas porosity. They occur when air or gas inside the mold cavity cannot escape through the molding sand and gets trapped in the final casting. The major sources of gas evolution include dissolved gases in the molten metal, vaporization of mold sand moisture and the combustion of binders in the mold sand or core. Reason of gas entrapment is high gas generation rate, poor permeability of sand, filling and solidification of molten metal is too fast and poor venting of the mold.

In order to get sound casting, during mould filling the flow of molten metal is to be properly controlled otherwise it creates the pouring related defects discussed above which is not acceptable at all. This can be obtained by a well designed gating system.

1.4 Organization of Report

The current investigation deals with a systematic methodology for optimization of gating system of castings at the simulation stage itself, so that sound castings can be produced during actual production.

This report is organized in six chapters. First chapter gives a brief introduction about gating system elements, types of gating system and filling related defects. Second chapter includes literature survey, consisting of related work in gating optimization and some guidelines for designing gating system. Third chapter includes motivation, goal, objectives, approach and scope of the project. Fourth chapter describes the proposed gating design optimization methodology, which includes formulation of objective function and formulation of various constraints like pouring time, ingate modulus, mold erosion, Reynolds number and quick filling that limits the filling rate of molten metal in the casting cavity. The flow chart for the gating optimization and design is also presented. Chapter five includes the implementation of the methodology using a case study along with results and discussions. Finally in the last chapter conclusions and future work are presented.

Chapter 2

Literature Survey

In the analysis of fluid flow in gating systems and the design of gating systems two approaches have been adopted: (1) hydraulics based analysis, involving solution of mass and energy conservation relations, and (2) a numerical analysis, involving solution of the mass and momentum conservation relations. The first section describes hydraulic based analysis on gating optimization. This section presents mathematical modeling, a case study and a nonlinear optimization of gating design. The second section describes numerical analysis approach, which includes governing equations, mathematical formulation and case study. The third section describes guidelines for designing the gating system. The fourth section includes gating location and optimization. The last section summarizes literature review.

2.1 Hydraulics based Analysis

A key requirement in the application of optimization to design is a computationally efficient mathematical model of the process representative involving the relationship between the design parameters. This is a principal reason for adopting the macroscopic, control volume, integral equation approach or hydraulics - based formulation of fluid flow, instead of the differential equation formulation, which requires a time-consuming solution of continuity and momentum equations.

The pipe-node-path representation of a gating system utilized in the hydraulics model formulation facilitates the incorporation of flow simulation and solids modeling algorithms within an object-oriented framework. Furthermore, well-established experimental techniques developed in the hydraulics field can be applied to the determination of loss coefficients for characterizing energy losses in complex-shaped bends and junctions of the type commonly encountered in industrial gating systems.

2.1.1 Mathematical Formulation

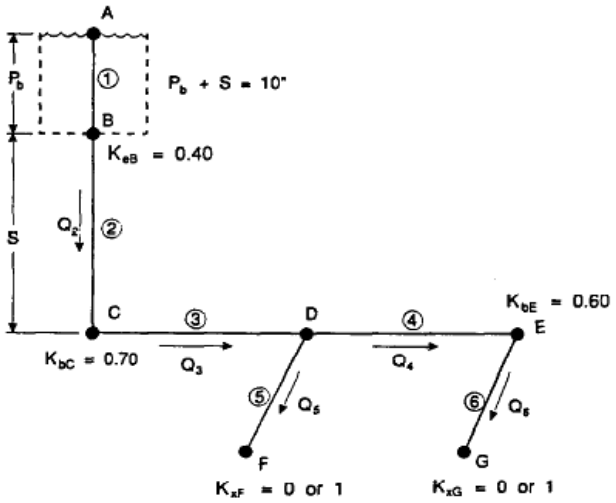

Figure 2.1: Representation of horizontal gating system (Kannan, 1991)

Figure 2.1 shows a schematic of a pouring basin plus sprue /single runner/ two-ingate horizontal gating system. The approach is to represent a gating system as an assembly of pipe segments connected at nodes (nodes C through G lie in the same horizontal plane). Individual pipe segments are identified by number and nodes by letter. The pipe / node representation proposed by Kannan S [1] facilitates data input and automatic assembly of the system of energy balance and continuity equations governing flow in the gating system.

Model formulation consists of writing an energy balance equation for each path in the system and a continuity equation for each node. A path is defined as a route that originates at the top of the sprue, follows connected pipe segments, and ends at an ingate, while encountering a given node at most once along the way. The number of paths in a gating system is equal to the number of ingates.

To write the continuity equations, it is necessary to define a convention for positive flow. The positive flow direction in a pipe segment is the direction of flow that will cause fluid to exit at an ingate. Consequently, as indicated in figure 2.1, it is assumed that divided flow occurs at node *D*. Combined flow is possible at this junction if Q_4 or Q_5 is negative. Whether divided or combined flow occurs at node *D* will depend on the heads at nodes C, *F,* and G, and the losses in connecting legs. In general, the steady-state energy equation from flow section *i* to flow section *j* along a stream tube can be expressed as,

$$\Delta H_{ij} = H_i - H_j = \sum (H_l)_{ij} \qquad (2.1)$$

Where ΔH_{ij} = the change in mechanical energy head along the stream tube between flow sections *i* and *j, H_i* and H_j are the total mechanical energy heads at flow sections *i* and *j*, and $\sum (H_l)_{ij}$ is the sum of the energy head losses along the stream tube between *i* and *j*.

The total mechanical energy head at a flow section is given by

$$H = z + \frac{P}{\gamma} + \frac{U^2}{2g} \qquad (2.2)$$

Where z, *P,* and U are the elevation, pressure, and velocity at the flow section, y is the specific weight of the fluid, and g is the acceleration due to gravity.

Energy head losses are of two main types, friction losses (H_f) and component losses (H_l) associated with changes in cross-section and/or direction of flow. Although the latter type of loss often dominates, friction losses may be significant in gating systems of larger castings. With reference to figure 2.1, four types of component losses arise in the general formulation of the two-ingate problem: (1) entrance loss at node B (H_{eB}); (2) bend losses at nodes C and *E* (H_{bC}, and H_{bE}); (3) junction losses at node *D* (H_{d34} and H_{d35}); and (4) exit losses at nodes *F* and G (H_{xF} and H_{xG}). Subscripts f, e, *b, d,* and x denote friction, entrance, bend, divided, and exit losses, respectively.

Head losses are expressed in terms of velocity U and loss coefficient K as

$$H_l = K_l \frac{U^2}{2g} \qquad (2.3)$$

For entrance, exit, or bend losses, the largest mean velocity in the pipe segments connected to the node is used to determine the head loss of the component. As indicated by Miller [2], any increase over and above the normal friction loss, arising from the redistribution of velocity and turbulence after the component, is included in the component head loss coefficient. The notation used for dividing *"T"* junctions is shown in figure 2.2. The loss coefficient *Kij is* defined as the ratio of the total head loss between leg *i* and *j* to the mean velocity head in leg *i* that carries the total flow (always referred to as leg 3). Figure 2.2 also shows the variation of loss coefficients K_{31} and K_{32} for sharp- flow edged 45° and 90° dividing "T"s-with flow ratio Q_1/Q_3 for the case of $A_1 = A_2 = A_3$. For the case ***of A1#A3 = A2***

(i.e., constant runner diameter), Gardel [3] obtained the following empirical relation for the dividing flow

$$K_{32} = 0.03(1-q)^2 + 0.35q^2 - 0.2q(1-q) \tag{2.4}$$

and

$$K_{31} = 0.95(1-q^2) + q^2\left[\left(1.3\tan\frac{\Phi}{2} - 0.3 + \frac{(0.4-0.1a)}{a^2}\right)\left(1-0.9\left(\frac{r}{a}\right)^{1/2}\right)\right] + 0.4q(1-q)\left(\frac{1+a}{a}\tan\frac{\Phi}{2}\right) \tag{2.5}$$

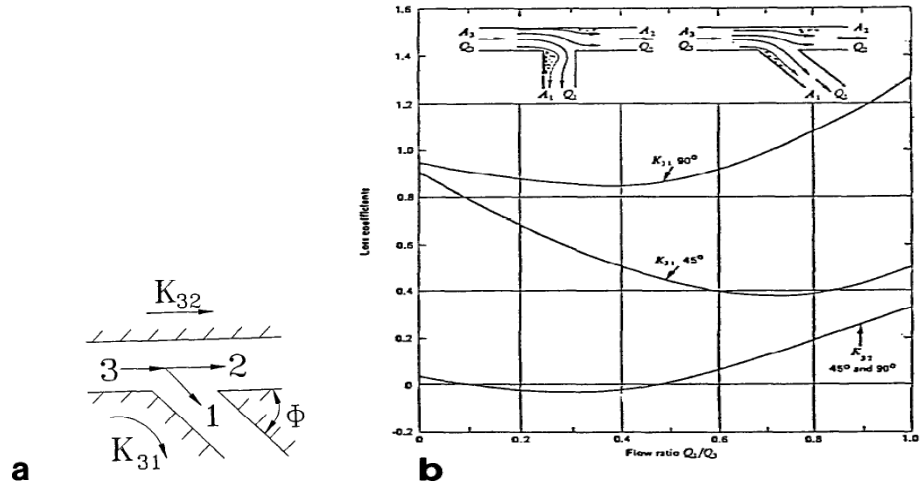

Figure 2.2 : (a) Convention for the loss coefficients for the dividing "T" junction and (b) loss coefficients for the sharp edged 45° & 90° dividing "T"s (Benedict,1980)

where $q = Q_1/Q_3$, $a = A_1/A_3$, r = fillet radius, and Φ= angle between leg 2 and leg 1. For the two-ingate case being considered, $K_{d35}=K_{31}$ and $Kd_{34} = K_{32}$. In the case of friction losses, the loss coefficient is given by

$$K_f = f\frac{L}{D} \tag{2.6}$$

where f is the friction factor, ***L*** is the length of the pipe segment, and ***D*** is the pipe diameter in the case of circular cross-section or hydraulic radius otherwise. The friction factor f is, in general, a function of the Reynolds number (*Re*) and the relative roughness of the pipe. For example, the Blasius equation

$$f = 0.316 \times \mathrm{Re}^{-0.25} \tag{2.7}$$

which is applicable for the case of turbulent flow in smooth pipes, has been used to estimate friction losses in gating systems with extended runners such as those for large steel castings. Model formulation for the two-ingate problem proceeds as follows. The two energy balance equations for Path I ***(A-B-C-D-F)*** and Path II ***(A-B-C-D-E-G)*** and the continuity equations for nodes ***B, C, D,*** and ***E*** are respectively given by following equations

$$H_A - H_F - H_{eB} - H_{bC} - H_{d35} - H_{xF} - \sum \left(H_f\right)_l = 0 \tag{2.8}$$

$$H_A - H_G - H_{eB} - H_{bC} - H_{d34} - H_{bE} - H_{xG} - \sum \left(H_f\right)_l = 0 \tag{2.9}$$

$$Q_1 - Q_2 = 0 \tag{2.10}$$

$$Q_2 - Q_3 = 0 \tag{2.11}$$

$$Q_3 - Q_4 - Q_5 = 0 \tag{2.12}$$

$$Q_4 - Q_6 = 0 \tag{2.13}$$

With the aid of equation (2.3) and the relationship Q = ***U*** . ***A,*** the energy balance equations can be expressed in terms of flow rate Q as follows

$$\left(z_A + \frac{P_A}{\gamma} + \frac{Q_1^2}{2gA_1^2}\right) - \left(z_F + \frac{P_F}{\gamma} + \frac{Q_5^2}{2gA_5^2}\right) - K_{eB}\frac{Q_2^2}{2gA_2^2} - K_{bC}\frac{Q_2^2}{2gA_2^2} - K_{d35}\frac{Q_3^2}{2gA_3^2} - K_{xF}\frac{Q_5^2}{2gA_5^2} - \sum_I f_i \frac{L_i}{D_i}\frac{Q_i^2}{2gA_i^2} = 0 \tag{2.14}$$

$$\left(z_A + \frac{P_A}{\gamma} + \frac{Q_1^2}{2gA_1^2}\right) - \left(z_G + \frac{P_G}{\gamma} + \frac{Q_6^2}{2gA_6^2}\right) - K_{eB}\frac{Q_2^2}{2gA_2^2} - K_{bC}\frac{Q_2^2}{2gA_2^2} - K_{d34}\frac{Q_3^2}{2gA_3^2} - K_{bE}\frac{Q_4^2}{2gA_4^2} - K_{xG}\frac{Q_6^2}{2gA_6^2} - \sum_{II} f_i \frac{L_i}{D_i}\frac{Q_i^2}{2gA_i^2} = 0 \tag{2.15}$$

In writing the bend loss expressions for nodes C and *E* in equations (2.14) and (2.15), it is assumed that the geometry of the system is such that $U_2 > U_3$ and $U_4 > U_6$.

Formulation for the two-ingate problem results in a consistent set of six equations (2.10)-(2.15), which are to be solved for the six unknown rates (Q_i) in each pipe segment. In general, for the case of constant friction factor, the continuity equations (2.10) - (2.13) are linear and the energy balance equations (2.14) and (2.15) are quadratic, reflecting the flow rate squared term. If Gardel's equations [3] are used to estimate junction losses and the Blasius equation [4] for friction losses, additional nonlinearities are introduced.

The system of equations is solved using the Newton-Raphson algorithm. Let $\vec{Q} = (Q_1 \ldots Q_6)$ denote the solution vector. Neglecting second-order and higher terms, a Taylor series expansion of each function f_i in the neighborhood of $\vec{Q}$ results in a set of linear equations for the corrections $\delta\vec{Q}$ that can be expressed as

$$\sum_{J=1}^{N} \alpha_{ij} \delta Q_j = \beta_i \tag{2.16}$$

Where

$$\alpha_{ij} = \frac{\partial f_i}{\partial Q_j} \qquad \beta_i = -f_i \tag{2.17}$$

Lower-Upper triangular matrix decomposition (Crout's method) is used to solve matrix equation (2.16) to obtain the corrections that are added to the previous solution vector to obtain the new solution,

$$Q_i^{New} = Q_i^{old} + \delta Q_i \quad i = 1,2,.....n \tag{2.18}$$

The algorithm is started with an initial guess of the solution vector, and the iteration process continues until the convergence criterion is satisfied. The convergence criterion can be expressed in terms of the magnitudes of the functions f_i or absolute values of the corrections δQi. An initial guess of $Q_i = 1 \times 10^{-4}$ m^3/s and convergence criteria of $\delta Qi/Qi = 1 \times 10^{-5}$ for each pipe segment were used in obtaining the simulation results.

For well vented, top-gated castings the assumption of steady state flow is reasonable, and the set of equations formulated above can be solved to directly obtain flow distribution through individual ingates and estimate mold-tilling time for a given casting volume. However, in the more general case of parting line or bottom-gated castings, the level of molten metal in the mold cavity will at some point rise above the ingates, thus creating a back pressure that tends to reduce the rate of flow into the mold cavity. In addition, if the mold is not properly vented, a significant gas pressure may develop and also act to retard the rate of flow into the cavity.

To get good results a *quasi steady-state approach* is used to handle time-dependent flow during mold filling. In writing the energy balances for the case of time-dependent flow during mold tilling, the termination point for both paths I and II is a node located on the mean

level of molten metal in the mold cavity, say node *H.* The change in molten metal height in the mold cavity, ΔZ_H, during time step Δt is dependent on the total volume of molten metal entering the mold cavity and the geometry of the mold cavity.

Consider the filling of a two-ingate bottom-gated rectangular mold cavity of constant cross-sectional area *A,* i.e., *A = f (z).* In the quasi steady-state approach, steady state conditions are assumed to hold during the time step and the system of equations solved to obtain the total flow rate into the mold cavity for arbitrary time step *i*, $Q^i_T = Q^i_5 + Q^i_6$. The volume of molten metal entering the mold cavity during the time step is $\Delta t.Q^i_T$, and the change in molten metal level is $\Delta Z_H = (\Delta t * Q^i_T)/A$. After each time step, the level of molten metal in the mold cavity increases by increments according to

$$z_H^{new} = z_H^{old} + \frac{Q^i_T \Delta t}{A} \tag{2.19}$$

the energy balance equations reformulated using z_H^{new} for the potential head in the mold cavity, and the system of equations solved to obtain the new total flow rate for the next time step. This process is repeated until mold filling is completed.

In general, the exit loss coefficients associated with the ingates (K_{xF} and K_{xG}) will increase from 0 to 1 during mold filling, with the value of 0 corresponding to discharge to atmosphere and the value of 1 corresponding to discharge into an infinite reservoir. Pressure differentials that are present in vacuum casting and other specialty casting processes, as well as back pressure associated with gases in the mold cavity, can be accounted for in the pressure head terms, P_F/γ and P_G/γ.

2.1.2 Example

An experimental model was built by Armour Research Institute [5] to simulate the flow on water modeling having circular cross sectional glass pipe. The set up was as shown in the figure 2.3. From 100 to 300 lb of molten steel at 2950°F were poured through the gating system depending on the particular test.

A small dam was located at the end of each gate to ensure that the gate would be filled with metal throughout the entire test. Junction losses were evaluated using Gardel's equation[3] and friction losses were assumed to be negligible.

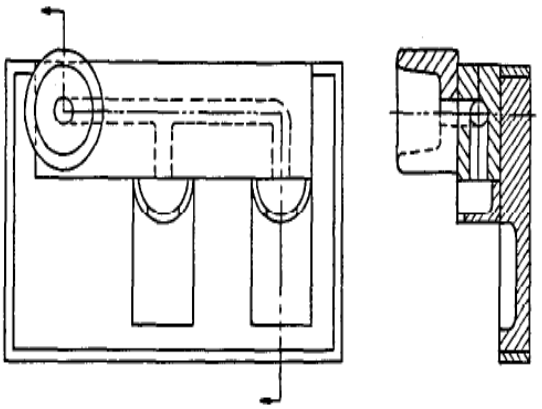

Figure 2.3(a) Experimental set up (Armour institute, 1951)

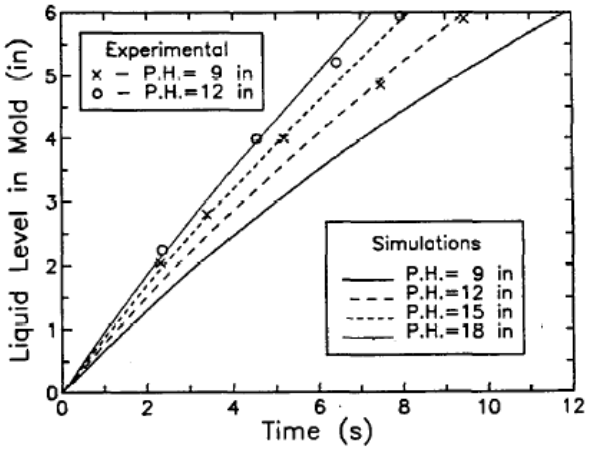

Figure 2.3(b) Results of Armour experiment

The Armour experimental results for molten steel (indicated by the open circles) and water modeling experimental results (indicated by the solid squares) are also plotted in figure 2.4**.**

The discrepancies between model-predicted and experimental flow distribution and mold-filling results are attributed primarily to uncertainty in the magnitude of the loss coefficients.

2.1.3 Nonlinear Optimization of Gating Design

In the analysis of fluid flow the goal is to solve for the flow rates Q_i in each pipe segment I given the geometry and loss coefficients for the system. Alternatively, from the standpoint of optimization of gating design, the goal is to select the best combination of gating component dimensions subject to the constraints of the problem.

In general, optimization determines a vector of design parameters $\vec{X}$, that maximizes or minimizes some aspect of the process represented by an objective function, *F(z)*, subject to specified constraints.

A typical objective function for gating design is casting yield, which is maximized when the total volume of the gating system, V_G**,** is minimized. Let V_i represent the volume of component i in the gating system so that $V_G = \Sigma V_i$ **.**

Typical constraints in gating design involve potential head z (where $z = P_b + S$ in figure 2.1)**,** mold filling time t_f, flow distribution through the ingates, and gating ratio.

With reference to figure 2.1, an example formulation of the optimization problem for gating design is given by

Minimize

$$F(\vec{x}) = \sum V_i \tag{2.22}$$

Subject to constraints

$$Z_1 \le z \le Z_2 \tag{2.23}$$

$$t_f \le t_f^* \tag{2.24}$$

$$A_3 - A_2.A_R^* = 0 \tag{2.25}$$

$$(A_5 + A_6) - A_2.A_G^* = 0 \tag{2.26}$$

$$Q_6 - (Q_5 + Q_6).Q_6^* = 0 \tag{2.27}$$

where the vector of design parameters is $\vec{X}$ = (z, A_2, A_3, A_4, A_5, A_6), and Z_1, Z_2, t_f*, A_R*, A_G* and Q_6* are design related constants. A sequential quadratic programming (SQP) algorithm is now being assessed for the solution of the nonlinear optimization problem formulated above.

2.2 Numerical Analysis

In numerical analysis based approach continuity, momentum and energy equations in differential form are solved using Marker and Cell (MAC) and Solution Algorithm Volume of Fluid (SOLA-VOF) to get point wise velocity, pressure and temperature field. All these methods divide mold model into a number of rectangular cells, which are classified as empty, full of surface cells. The results obtained at each time step are used to simulate the flow of molten metal in the mold cavity. The simulator is then coupled with optimization techniques considered for the analysis, which iteratively finds a search direction that guarantees a better design in every step. The procedure terminates with a design that is optimal with respect to the design variables considered in optimization process.

2.2.1 Governing Equations

Molten metal during mold filling follows the three basic fundamental equations of mass, momentum and energy balance. These equations, expressed in a differential form and referred to as Navier-Stokes equations, are given below.

(1) Continuity equation

$$\frac{\partial \rho}{\partial t}+\frac{\partial}{\partial x_j}(\rho v_x)+\frac{\partial}{\partial x_j}(\rho v_y)+\frac{\partial}{\partial x_j}(\rho v_z)=0 \tag{2.28}$$

(2) Momentum Equation

$$\rho\left[\frac{\partial v_x}{\partial t}+v_x\frac{\partial v_x}{\partial x}+v_y\frac{\partial v_x}{\partial y}+v_z\frac{\partial v_x}{\partial z}\right]=-\frac{\partial p}{\partial x}+\mu\left[\frac{\partial^2 v_x}{\partial x^2}+\frac{\partial^2 v_x}{\partial y^2}+\frac{\partial^2 v_x}{\partial z^2}\right]+\rho g_x=0 \tag{2.29}$$

$$\rho\left[\frac{\partial v_y}{\partial t}+v_x\frac{\partial v_y}{\partial x}+v_y\frac{\partial v_y}{\partial y}+v_z\frac{\partial v_y}{\partial z}\right]=-\frac{\partial p}{\partial y}+\mu\left[\frac{\partial^2 v_y}{\partial x^2}+\frac{\partial^2 v_y}{\partial y^2}+\frac{\partial^2 v_y}{\partial z^2}\right]+\rho g_y=0 \tag{2.30}$$

$$\rho\left[\frac{\partial v_z}{\partial t}+v_x\frac{\partial v_z}{\partial x}+v_y\frac{\partial v_z}{\partial y}+v_z\frac{\partial v_z}{\partial z}\right]=-\frac{\partial p}{\partial z}+\mu\left[\frac{\partial^2 v_z}{\partial x^2}+\frac{\partial^2 v_z}{\partial y^2}+\frac{\partial^2 v_z}{\partial z^2}\right]+\rho g_z=0 \tag{2.31}$$

(3) Energy equation

$$\frac{\partial T}{\partial \tau}+v_x\frac{\partial T}{\partial x}+v_y\frac{\partial T}{\partial y}+v_z\frac{\partial T}{\partial z}=\frac{K}{\rho C_v}\left[\frac{\partial^2 T}{\partial x^2}+\frac{\partial^2 T}{\partial y^2}+\frac{\partial^2 T}{\partial z^2}\right]=0 \tag{2.32}$$

(4) Volume of fluid (VOF)

$$\frac{\partial F}{\partial t}+v_x\frac{\partial v_x}{\partial x}+v_y\frac{\partial v_y}{\partial y}+v_z\frac{\partial v_z}{\partial z}=0 \tag{2.33}$$

In the above equation if density is assumed to remain constant then we have four unknown velocities $\left(v_x, v_y, v_z\right)$ and pressure (p) and we have four equations. The solution of equations yield point wise velocity and pressure fields rather than values averaged at inlets and outlets as in case of hydraulic based analysis. The solution is repeated for each time step considered. Finally the results are processed and displayed graphically to visualize the flow front through casting.

Carlos et al. [6] solved these set of equations using numerical differentiation technique. A commercial software package FLOW3D was directly used to simulate the results obtained after each time step. This package utilizes Solution Algorithm-Volume of Fluid (SOLA-VOF) as one of the finite difference methods. He used Sequential Quadratic Programming (SQP) as the optimization technique for his experiment. To accomplish this optimization VisualDOC was used as the tool to optimize gating system design. The experimental set up was as shown in figure 2.6.

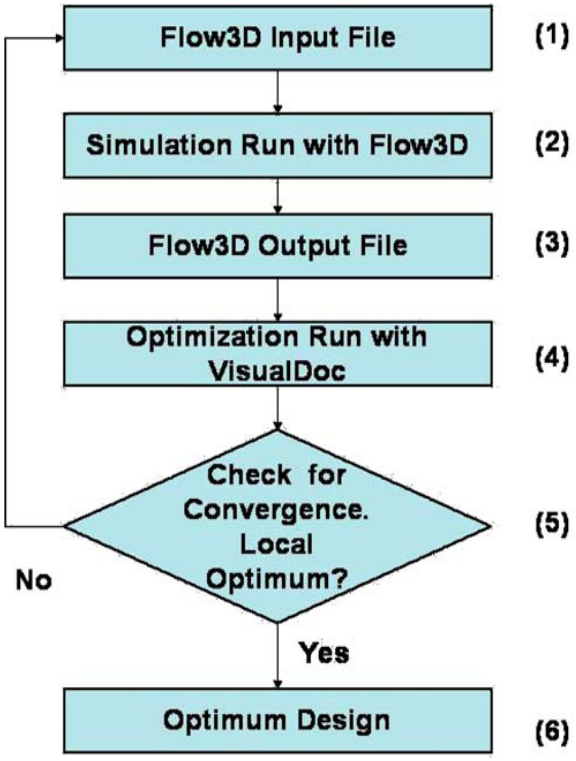

Figure 2.5 Flow-chart of the overall optimization process (Carlos et al.,2006)

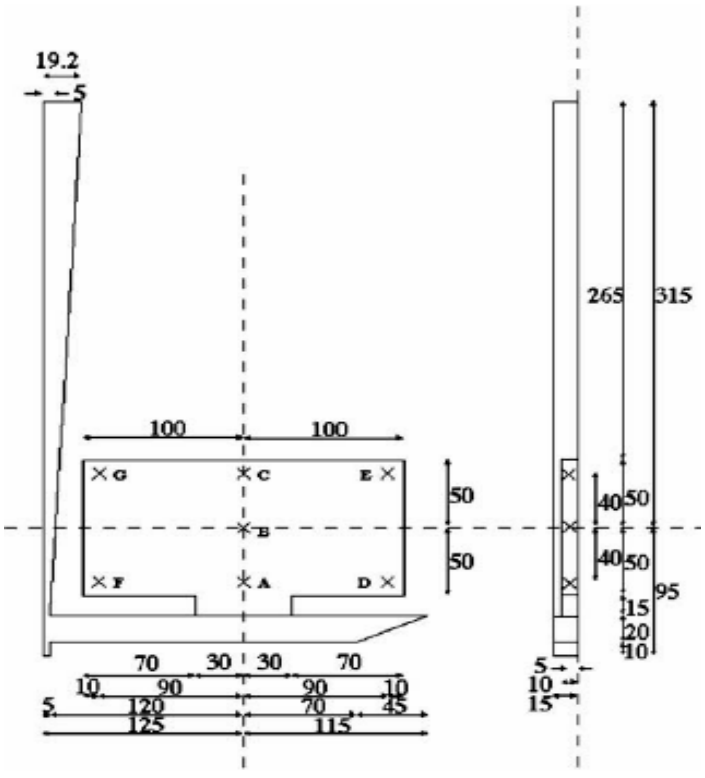

Figure 2.6 Drawing of gating system, units, mm (Sirrell,1996)

2.2.2 Mathematical Formulation

The optimization model proposed by Carlos et al. [6] is as follows:

Design Variables are

ZL = runner depth and

CX = slope of the runner tail

$$Minimize\ V_j(ZL, CX) = \sqrt{V_{xj}^2 + V_{yj}^2 + V_{zj}^2}$$

$$subject\ to:$$

$$t_{ci} \le t_{ej} \qquad i \in I, j \in J$$

$$ZL_i \le ZL \le ZL_u$$

$$CX_l \le CX \le CX_u$$

2.2.3 Example

Carlos et al. [6] is the first to optimize 3D gating system design. For their experimental design (DOE), a Taguchi L9 array was used. The complete set of analysis includes two design factors (ZL & CX) and three levels in the tabular form it is written as follows.

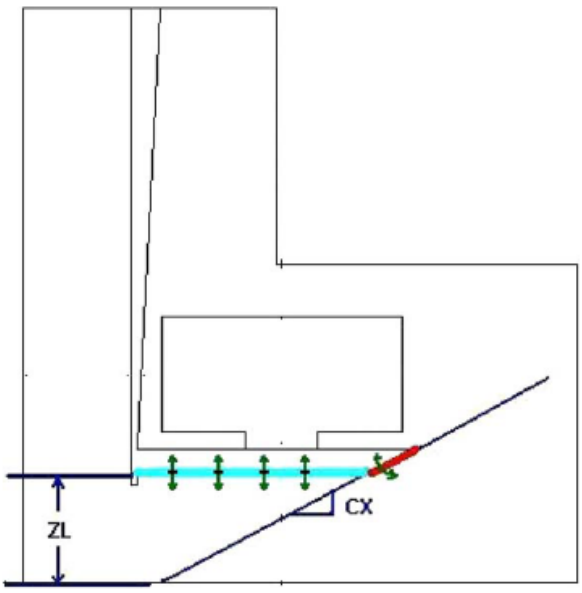

Figure.2.7 Design variable representation (Carlos et al.,2006)

For the experimental design Taguchi L_9 array was used. The complete set of analysis for the first experiment includes 27 executions, using 3 factors at 3 levels each ($3^3 = 27$). The result from the first experimental presents a best value of step size (SS) in between 1×10^{-2} and 1×10^{-5}. The second set of experiments now conducted using 2 factors at 3 levels each ($3^2 = 9$) for a fixed value of SS = 1×10^{-4}. It is given in the following table.

Analysis No.	ZL	CX
1	9.5	0.3
2	9.5	0.9
3	9.5	1.5
4	10.25	0.3
5	10.25	0.9
6	10.25	1.5
7	10.8	0.3
8	10.8	0.9
9	10.8	1.5

ZL in cm

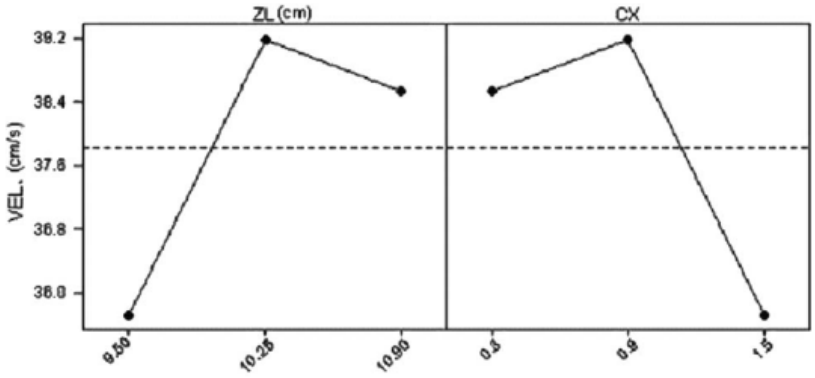

Figure 2.8 Main effect of design variables (Carlos et al.,2006)

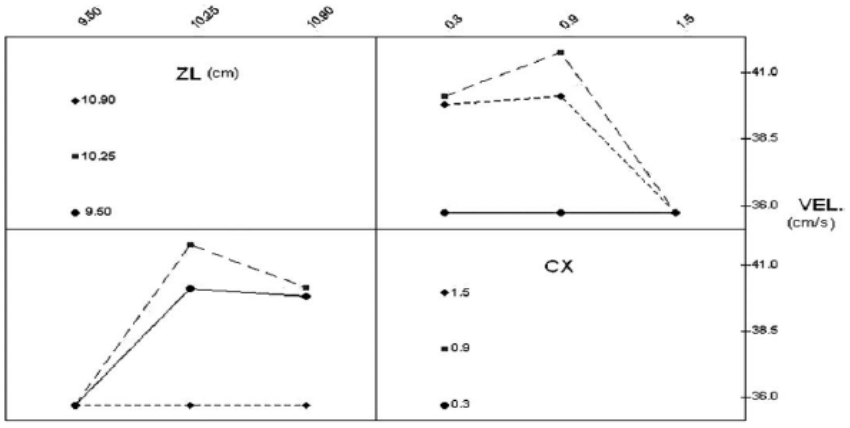

Figure 2.9 Interaction effects between design variables (Carlos et al.,2006)

Figure 2.8 shows the effect of initial value of design variable on the response. It is clear that starting ZL at low & CX at high value results in better performance. From the figure 2.9 the use of lower value of ZL (9.5), helps to obtain a better design that minimizes ingate velocity irrespective of the value of CX used. Similarly setting the value of CX at 1.5 irrespective of the ZL value enhances the performance. Figure 2.10 shows a 3-D plot of initial values of design variables *versus* ingate velocity. It can be seen that at lower & upper values of the design variables resulting in four combinations of ZL & CX values (9.5,0.3;9.5,1.5;10.9,0.3& 10.9,1.5) gives optimal design.

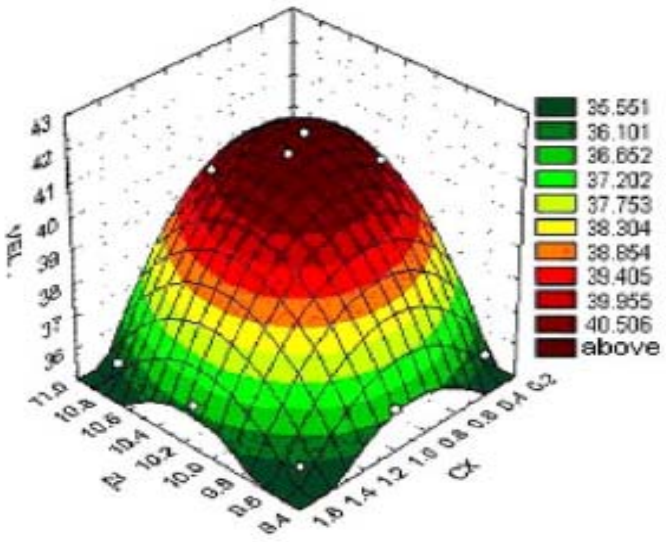

Figure 2.10 Iteration between initial values of design variables ZL and CX to minimize ingate velocity of molten metal (3-D plot) (Carlos et al.,2006)

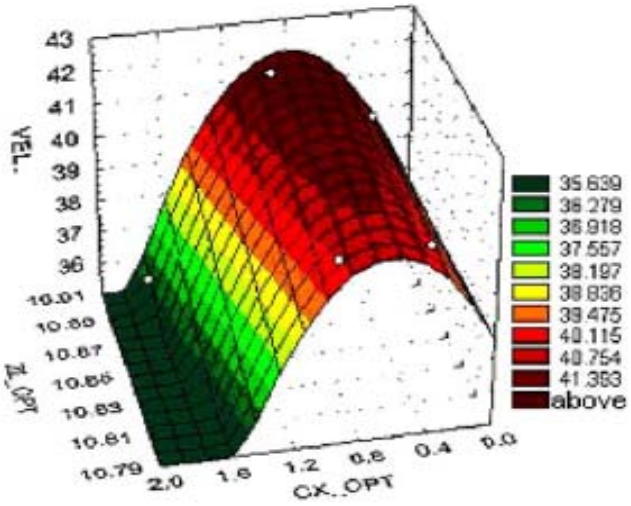

Figure 2.11 Final values of design variables ZL_opt and CX_opt to minimize ingate velocity of molten metal (3-D plot) (Carlos et al.,2006)

From figure 2.11, optimized gating system includes a ZL value between 10.91 and a CX value higher than 1.5. With this values, velocity lies between 35.6 and 37.6 cm/s. A comparison between the results obtained using the original runner vs. the optimum design was carried out using the foundry criteria. Figure 2.12 shows the original gating design when the ingate is activated, the aluminum goes into the mold cavity, and some air is trapped in the runner. Figure 2.13 shows the optimized gating design when the ingate is activated, the aluminum goes into the mold cavity, and there is not air trapped in the runner. This happened at filling time of 0.55 s.

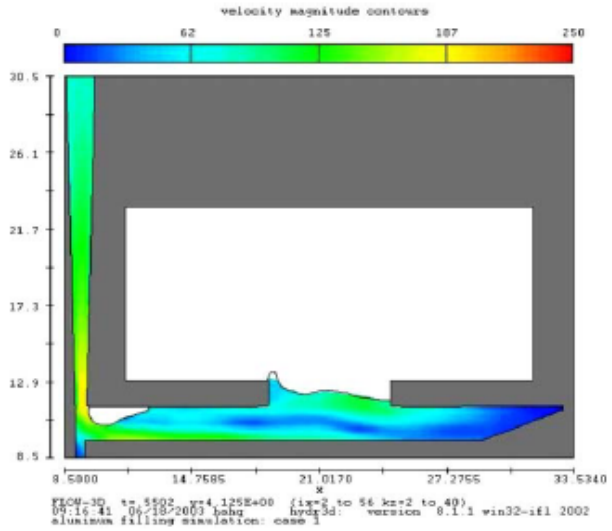

Figure 2.12 Velocity of molten Aluminium in the original gating design when ingate is activated (Carlos et al.,2006)

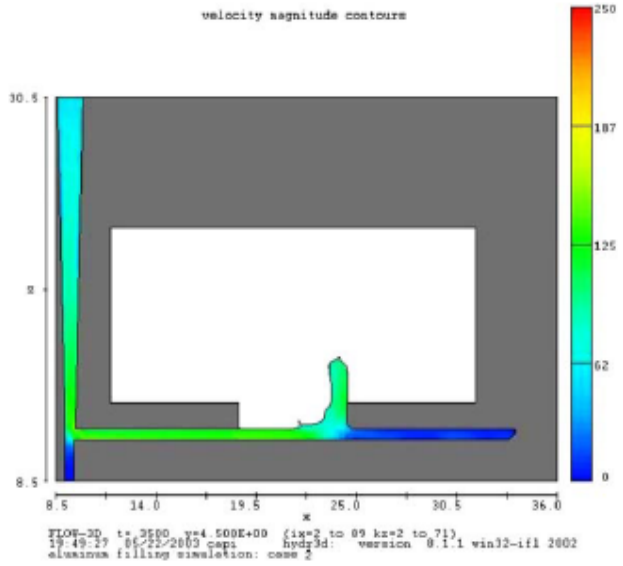

Figure 2.13 Velocity of molten Aluminium in the optimized gating design when ingate is activated (Carlos et al.,2006)

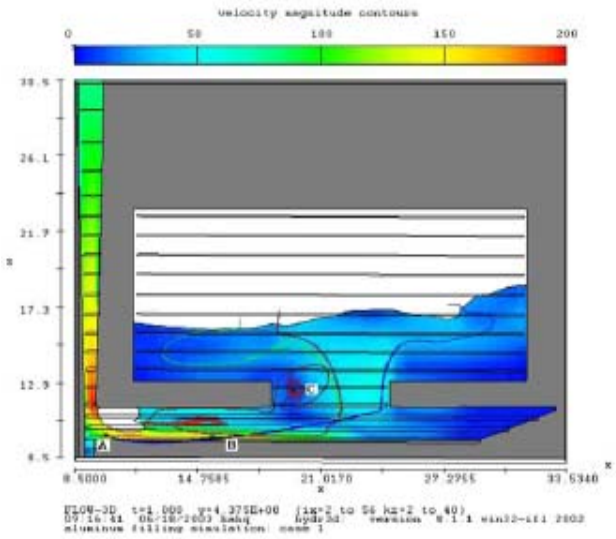

Figure 2.14 The tracers of particles A-C displayed with velocity of molten aluminium through original gating system at filling time of 1 sec (Carlos et al.,2006)

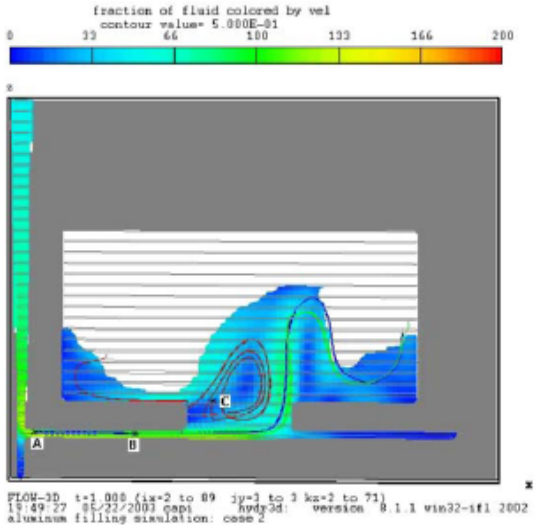

Figure 2.15 The tracers of particles A-C displayed with aluminum velocity through optimized gating system at filling time of 1 sec (Carlos E. Esparza et al.,2006)

Figure 2.14 shows the original gating design and three particle tracers, A–C. The tracers show the pathway that each of these particles follows within the aluminum stream movement. Tracer of particle C shows that some aluminum circulates back into the main runner as the system continues to fill up. Figure 2.15 shows the optimized gating design and three particle tracers, A–C. The tracers that the liquid moves forward progressively while the system continues to fill up (without returning to the main runner).

2.3 Guidelines for Designing Gating System

The guidelines for gating system design proposed by Ravi B [7], Ruddle R.W [8], Benedict R. P [9] and Campbell J [10,11] is given below.

- The size of the sprue fixes the flow rate. In other words, the amount of molten metal that can be fed into the mold cavity in a given time period is limited by the size of the sprue.
- The sprue should be located at certain distance from the gates so as to minimize velocity of molten metal at ingates. Often, the flow leaving the sprue box is turbulent; a longer path and a filter enable the flow to become more laminar before it reaches the first gate.
- Rectangular cross-section sprue is better than circular one with the same cross-sectional area, since critical velocity for turbulence is much less for circular sections. In addition, vortex formation tendency in a sprue with circular cross section is higher.
- Sprue should be tapered by approximately 5% minimum to avoid aspiration of the air and free fall of the metal.
- Ingates should be located in thick regions.
- Locate the gates so as to minimize the agitation and avoid the erosion of the sand mold by the metal stream. This may be achieved by orienting the gates in the direction of the natural flow paths.
- Multiple gating is frequently desirable. This has the advantage of lower pouring temperatures, which improves the metallurgical structure of the casting. In addition, multiple gating helps to reduce the temperature gradients in the casting.
- Rectangular cross section of runners and ingates are generally preferred in sand castings.
- Runner extensions (blind ends) are used in most castings to trap any dross that may occur in the molten metal stream.
- A relief sprue at the end of the runner can be used to reduce the pressure during pouring and also to observe the filling of the mold.

2.4 Gating Location and Optimization

To the best of our knowledge, there have been very few attempts to use optimization techniques for addressing the problem discussed here. The first published work showing an effort to apply a numerical methodology to optimize a gating system is due to Bradley and Heinemann [12] in 1993. They used simple hydraulic models to simulate the optimization of the gating during the filling of molds. Other published work related to gating optimization was carried out by McDavid and Dantzig [13,14] in 1998. Their simulation was 2 - dimensional (in terms of the mold geometry). Their approach also used a mathematical development addressing the design sensitivity. The simulator used was FIDAP, a FEM based program for flow simulation. No velocity constraints were imposed at the ingates.

Jong and Wang [15] described the optimal design of runner-system. Lee and Kim [16] used a modified complex method to reduce warpage by optimizing the thickness of different surfaces. Balasubramanian and Norrie [17] described a multi-agent system, with emphasis on integrating certain design and control functions in manufacturing and shop floor control activities. However, there is a scarcity of research articles on the application of a multi-agent system to resolve some of the common problems, especially the design of a riser and gating system in casting.

An optimum pouring time for steel castings is calculated by the experimental relation given by Lange and Bukowski [18]. Iyengar [19] presented a step-by-step procedure of a gating system design. A rough casting layout is first prepared and runner(s), gates and sprue are placed in a desired position. The different formulae given by him are based totally on the experimental results. He provided complete information about the runner, sprue and gates based on different calculations and finally designed the gating system of the casting. This research provides a strong base to combine the knowledge base pertaining to riser and gating design and thereafter develops an agent-oriented framework.

Ranjan et al. [20] developed a multi-agent framework for riser and gating system design for sound casting. Pandelidis et al. [21] developed a system that used MOLDFLOW for flow analysis. An objective function, the sum of a temperature differential term and the number of elements term, was used to represent quality of a gating design. The optimization was executed in two stages. In stage one, the optimum gate location was found by holding

molding conditions constant and evaluating the objective function values of all adjacent nodes to the current node. The node having the maximum improvement in the objective function became the new current node. This stage was executed until there was no improvement in the objective function. During stage two, the optimized gate location was kept constant and the moulding conditions were optimized.

Pandelidis and Zou [21] made several improvements on this method. A combination of simulated annealing and a hill climbing search scheme was used to find the optimum gate location in terms of minimizing the objective function. The parameters chosen were the above mentioned two parameters plus an additional one, namely frictional overheating.

Bose and Toussaint [22] introduced a method for determining the optimum gate location for a pin gate. Pure geometric characteristics were used to calculate the geometric centers of a given model, based on the assumptions that the maximum distance from the pin gate to any point in the mould and the maximum number of turns on the path from a point in the mould to the pin gate should be minimized. This method was only capable of analyzing models with simple 2D vertex polygon geometry, which are too simple for a practical application.

Saxena and Irani [23] proposed another method based on the geometrical features of the molding alone. The selection of optimum gate location was based on a gate location that would have the best compromise in terms of minimizing flow length while maximizing flow volume. The flow length was defined as the shortest distance from the gate to the extremities of the part, and the flow volume as the volume that the gate can feed in a defined region.

The above two pure geometric methods exclude many parameters that cannot be provided by geometric information alone. It should be noted also that defining flow length solely using geometric information might not reflect the flow path in the real filling process. Thus the quality of the solution cannot be guaranteed.

To overcome the difficulties of the geometrical approach, Ong et al. [24] utilized a knowledge base system for gate selection. Four types of information were utilized: mould data, material data, product description and product specification. Subsequently, an Artificial

Intelligence (AI) system was used as a rating system to determine the optimum gate location with the desired criteria.

Mehl et al. [25] used non-dimensional charts that incorporated information on flow length, thickness, flow velocity and material viscosity. The charts could be used to provide information on optimal gating schemes besides fillability and minimum part thickness. The purpose of this approach was to provide an analysis tool that address whole part design in the preliminary stages. It resembled a design guide than an optimum process. Relying on rule based or heuristic knowledge and charts, the above methods may offer quick solutions. However, they are unable to deal with complex moulds and high quality requirements, such as tight tolerances. Without filling analysis, it is difficult to perform proper optimization.

Irani et al.'s [26] AMDS system combined both geometry related parameters and process-related parameters for the objective function. There were two stages for gate optimization. During the first stage, evaluation of the candidates wall/edge primitives was based on three criteria, namely, the section thickness, flow volume and flow length. The objective was to determine the wall/edge among the candidates that had the greatest section thickness, largest flow volume and the shortest flow length. During the local search, from a filling analysis and knowledge based evaluation, the solution was improved upon until the best solution was found. It should be noted that in the system, many design constraints were considered as geometry-related parameters, such as aesthetic concerns, weld line location and strength, venting and flow direction, etc. However, the capability of this system was limited to very simple geometry, which was 2.5D parts made up of planar rectangular wall features.

Lee and Kim [27] argued that a warpage analysis was required to adequately encompass part quality in the objective function. Using maximum nodal displacements generated from warpage analyses, and also a trained neural network for calculating izod impact strength, their objective function incorporated aspects of warpage, structural integrity and weld line locations. The optimum gate location was selected using an adjacent node search after a feasible region had been selected. A degree of interaction was required in their method, as the feasible regions had to be first selected by the mould designer.

Young [28] proposed a searching procedure for composite molding. Based on minimizing an objective function defined by inlet pressures, temperature differences and

boundary filling times, genetic algorithm was employed. Through a comparison of this method with two other methods, namely hill-climbing and random search, the author found that genetic algorithms offered the best results without the cost of excessive computation time, although he conceded that solutions using genetic algorithms were only approximately optimal.

In their research toward automated cavity balancing, Lam and Seow [29] proposed a hill-climbing algorithm for the generation of flow paths. Subsequently, Lam and Jin [30] extended the hill-climbing algorithm for the generation of flow paths to 2.5D parts. Based on the 2.5D flow path generation, a gate optimization algorithm was developed. For gate optimization, two objective functions were investigated, namely (i) the minimization of the standard deviation of the flow lengths and (ii) the minimization of the standard deviation of boundary nodes' filling time. It was discovered that the minimization of the standard deviation of boundary nodes' filling time is more effective, especially for parts with varying thickness. Design constraints such as weld lines and aesthetic concerns were not considered.

However, in a practical gating design, there are many restrictions for gate location. For example, a two-plate mould is preferred for its low costs if the geometry and dimensional tolerance is not an important factor for the part, and usually edge gates will be used. Nevertheless, if tight dimensional tolerances are required, to achieve a better fill pattern and reduce warpage, top centre gating might be an improvement over edge gating, and the gating area can be expanded to the surface of the part not on the parting line. In this circumstance a three-plate mould is required. In both cases, the gate location must be further restricted when aesthetic requirements, weld/meld lines, and venting etc. are considered.

Considering the variety and complexity of the geometry models and constraints in a real design, together with the limited modeling tools provided by a CAE system, it is a formidable task to define and handle the constraints in a CAE system alone. It will be more convenient to define these constraints together with the geometrical information using CAD tools. However, translation of constraints from a CAD model into a CAE model, as well as feedback from the CAE optimization results to modify the CAD model are required. Both operations are laborious and error-prone. For practical gate optimization with design constraints, it is more promising to take advantage of an integrated CAD/CAE system.

Irani and Saxena [31] described a feature modeling utility (FMU) that coexisted with commercial CAD systems by providing external feature-based functionality and making it available to application programs. As no such kind of utilities was available at that time in the CAD modeling system, the FMU aimed to address the special requirement of modeling wire-frame, surface and solid features at the same time in a CAE-related application. It was built on the basis of two supporting technologies. The first was a non-manifold topology (NMT) representational scheme which could simultaneously support wire-frame, surface and solid modeling. The second was a software system, referred to as Topology and Geometric Modeling Utility (TAGUS), which incorporated NMT. It was built on top of common CAD modelers, providing a bridge between the CAD systems and CAE optimization applications. It should be noted that a separate TAGUS is not required now, because current CAD systems can handle the modeling of wire-frame, surface and solid features simultaneously.

Lam et al. [32] developed an automated gate optimization routine to handle the design constraints such as a no-gate constraint and an edge-gate constraint, taking an advantage of the functionalities of CAD and CAE operations. Standard deviation of filling time is used as the objective function during the gate optimization process.

Ravi and Srinivasan [33] developed a methodology for computer aided gating and metal rising simulation. A comprehensive study has been carried out for metal rising in the mold and graphically simulated. It takes into account the instantaneous flow rate and varying cross sectional area of the component to determine the filling rate.

2.5 Conclusions from Literature Review

- Hydraulics based analysis of gating system carried out by Kannan [1] is in good agreement with the experimental results, as viscosity of molten metal (Al – 0.0020, Mg – 0.0013, iron –0.0016, steel – 0.0014 in^2/sec) is close to water (water – 0.016).

- Numerical based analysis of gating system considered by Carlos and his team members uses Navier-Stokes equations of fluid. A process simulator like MAC, SOLA-VOF and Flow3D is used to solve this equation to get point wise velocity, pressure and temperature field at each time step. This is coupled with an optimizer for gating optimization. Though a very good improvement was arrived at by this

method, they used only two design variables for the optimization in his experiment namely runner depth and runner tail inclination angle. There are number of factors that affect the final gating design. So there is complete absence of any **robust design** procedure for high performance gating system. Therefore, theoretical modeling is essential.

- Literature on optimization of gating system recommends minimizing the ingate velocity of melt, maximizing the yield, minimizing warpage and optimizing location of ingate. However no one appears to have focused on the maximizing the filling rate of molten metal. This project focuses on the maximizing the filling rate with not to have a defect and satisfying other design constraints. Higher filling rate is useful to increase the production rate of castings. Higher filling rate is also required in thin and long castings which lose heat very rapidly. In these castings, it helps to avoid cold shut and misrun.

- From the various optimization techniques mentioned in literature on gating design, it is recommended to use Sequential Quadratic Programming. Because convergence rate is very fast and gives the optimized values of design variables with less number of iterations as compared with other optimization technique.

Chapter 3

Problem Definition

3.1 Motivation

Good casting quality is initially dependent on a good gating design. Common industry practice is to use the gating design based on trial and error approach by experimentation. Through an optimized gating can be obtained by this way, but it takes both time and money spent behind this project. By this project we can accelerate this experimentation using iterative approach to the solution considering all the parameters that influence the cast product quality and cost also. Moreover published research work has not concentrated on optimization of gating design based on maximum filling rate, which is critical in thin and long casting which loses heat rapidly to avoid defects like cold shut and misrun. High filling rate is also useful to meet the customer due date by increasing the production rate by this method.

3.2 Goal and Objectives

The goal of this project is "***to evolve a systematic methodology to optimize the gating system design for maximizing filling rate of molten metal in sand casting"***.

Objectives

- Identifying critical parameters in gating design that affect mould filling process including controllable (or design) factors and uncontrollable (or noise) factors that affect the gating design and hence final casting.
- Selecting a SQP optimization algorithm using the aforementioned design parameters.
- Implementing this algorithm using Matlab programming for optimizing the process parameters.
- Designing the gating system using optimized value of design variables.

3.3 Approach

In order to achieve the above mentioned objectives, the work is divided into three stages

1. In the first stage, literature and knowledge regarding gating design is acquired and is represented in the form of types of methods. The information is obtained from the standard hand books on metal casting, research papers, and consultants and from academia.
2. In second stage, various optimization techniques are studied and the best optimization technique implemented. The optimization technique implemented for maximization of filling rate is SQP (Sequential Quadratic Programming). Along with this the formulation of constraints that affect the process of filling is also formulated.
3. In final phase, new constraints that affect the filling process is formulated. Programming (coding) for optimizing the fill rate is also carried out. Finally the algorithm of SQP and the constraints formulated in the second and third stages will be implemented in the coding to optimize the fill rate.

3.4 Scope

The scope of the work is limited to optimize the gating system for sand casting only. This is because 90% of all casting produced are made by this process and it is applicable to both ferrous and non-ferrous metals.

Chapter 4

Proposed Gating Design Optimization Methodology

This chapter describes the proposed gating design optimization methodology. The first section of this chapter presents the overall methodology implemented for optimizing the gating dimensions. The second section deals with the objective function formulation for maximizing the filling rate of molten metal in the mold cavity. The third section includes a mathematical formulation of five constraints implemented for optimization. The five constraints deal with pouring time, ingate modulus, mold erosion, Reynolds number and quick filling.

4.1 Gating Design Optimization Methodology

The overall methodology implemented for optimizing the gating system is presented in figure 4.1.The necessary input for the methodology are dimensions of rectangular casting, material and mold properties, initial mold height. It is also necessary to specify the composition of mold (with respect to percentage of binder, additive, silica) and the properties of binder, sea coal, air and burnt gases. The second step is to define the objective function which is to maximize the filling rate of molten metal. The constraints for the above optimization are specified in the form of pouring time, modulus of ingate (with respect to the connected section), mold erosion, Reynolds number and quick filling. The formulation of objective function and the aforementioned constraints are described in the following sections. This optimization is solved using Sequential Quadratic Programming (SQP) technique. The algorithm and the source code have been given in appendix. The solution is run till convergence to obtain the optimized values of area of ingate and velocity of molten metal at ingate. A suitable gating ratio from reference [10] is used to calculate sprue and runner dimensions.

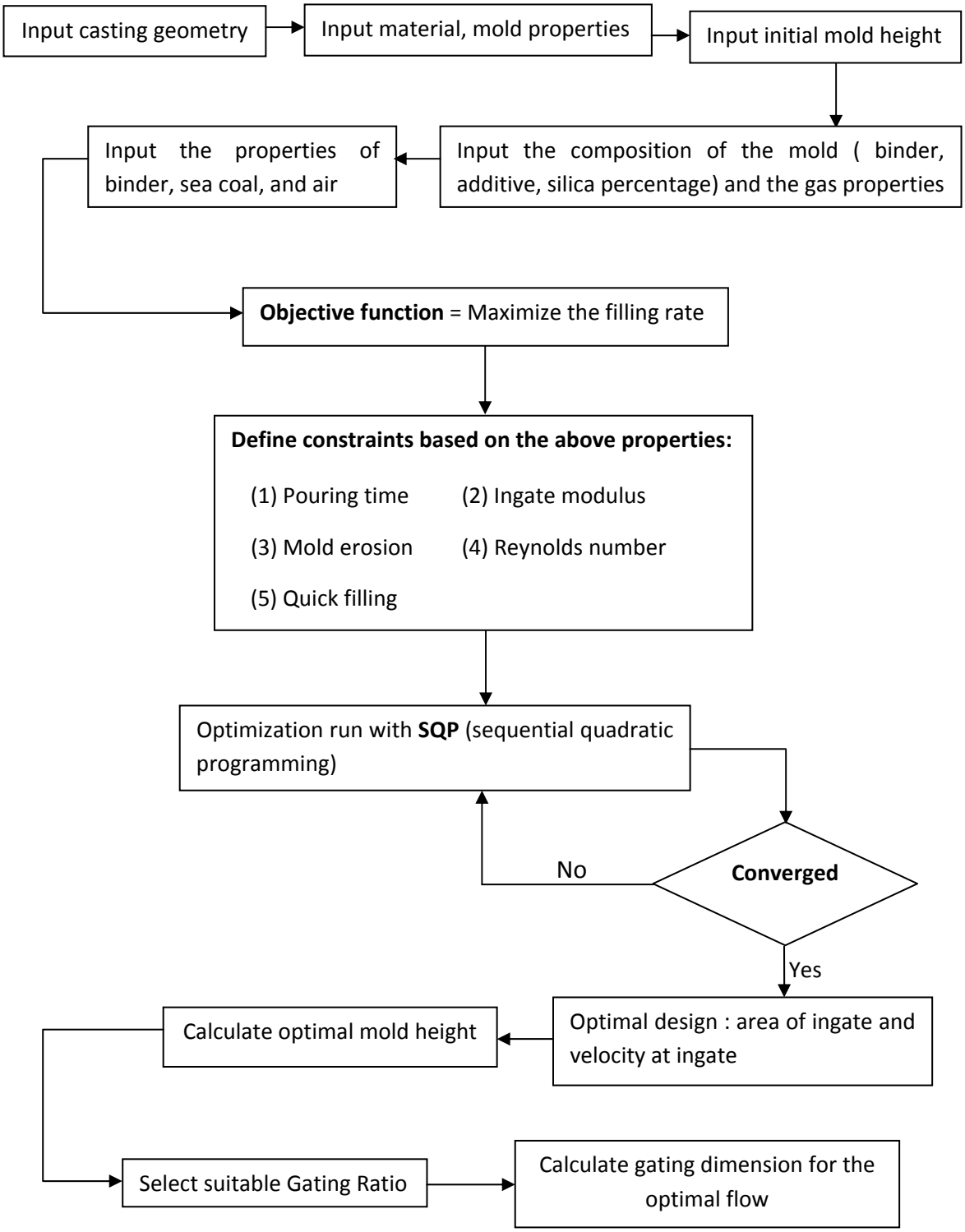

Figure 4.1 Gating design optimization methodology

4.2 Formulation of Objective Function

The objective function proposed is to maximize the filling rate of molten metal for sand casting.

Mathematically,

Filling rate = $\rho_m \times A_g \times V_g$

Where ρ_m = density of molten metal

A_g = cross sectional area of ingate

V_g = Velocity of molten metal at ingate

Hence, mathematically, objective function is given by

Objective function: maximize $\rho_m \times A_g \times V_g$ (4.1)

As the variation of density of metal above melting point temperature is very small, we can assume constant density of molten metal in our analysis. Therefore there are only two design variables (cross sectional area of ingate and velocity of molten metal at the ingate), which are taken into consideration for gating optimization.

4.3 Formulation of Constraints

A well designed gating system, satisfying the objective function of maximum filling rate, must be free from the pouring related defects like cold shut, misrun, higher turbulence, sand inclusion and gaseous entrapments. This can be achieved, if the following five constraints are satisfied: (1) pouring time, (2) modulus of ingate with respect to connected section, (3) mold erosion, (4) Reynolds number and (5) quick filling. These constraints are described in detail in this section.

4.3.1 Constraint 1 (Pouring Time)

As the molten metal is poured in the mold cavity, its temperature decreases with time. If fall in the molten metal temperature is sufficient to overcome the liquidus temperature line, molten metal will start solidifying.

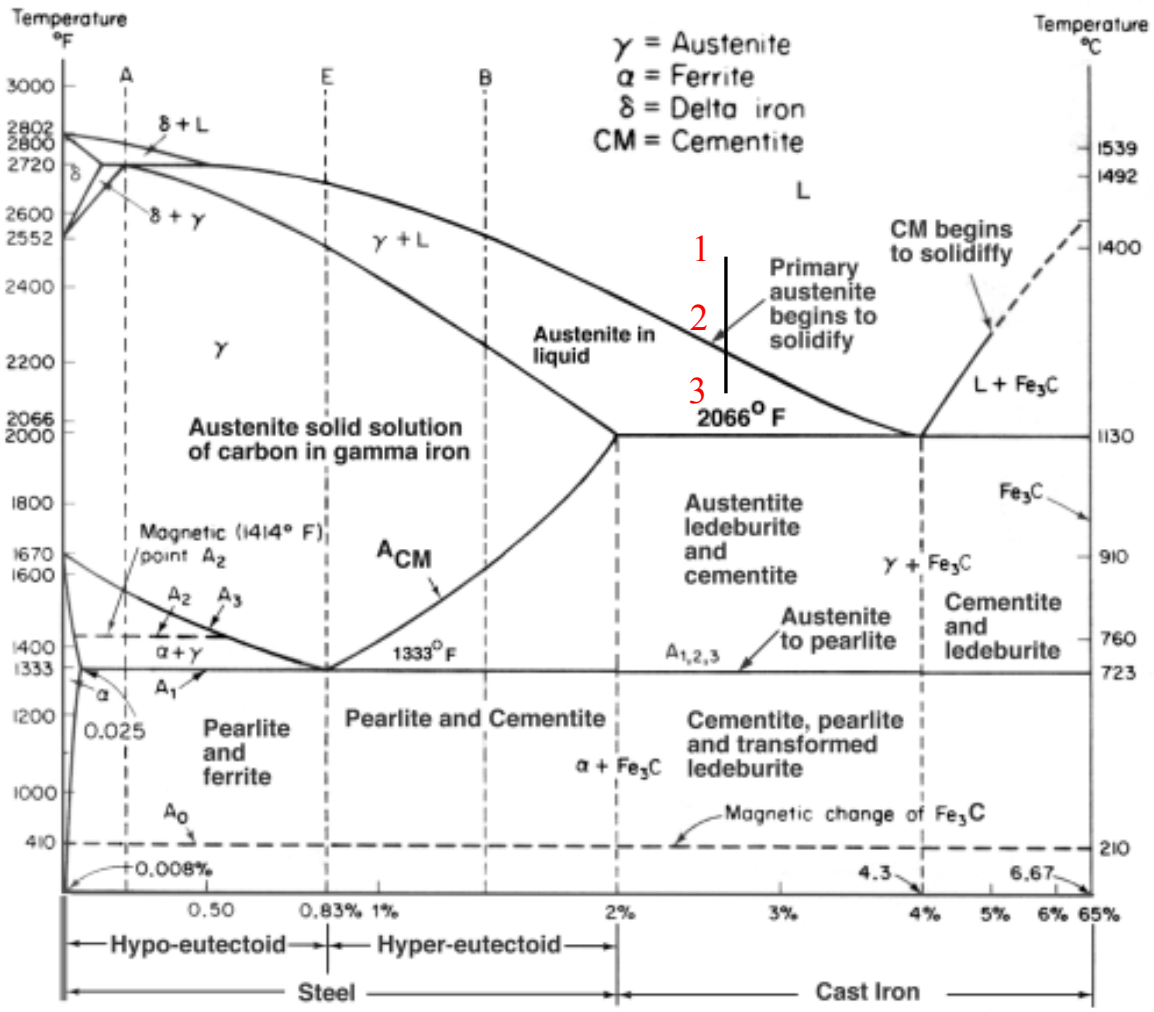

Figure 4.2 FeC diagram

For example figure 4.2 shows the FeC diagram. For the 2.77% of carbon the pouring temperature as indicated by data point-1 is 1400 ºC. It will decrease with time, so the temperature falls below 1400 ºC. When the temperature reaches to 1018 ºC, solidification starts.

If during pouring solidification starts, it results in cold shut and misrun defect in the final casting, which is unacceptable. So in order to have a sound casting solidification should not start until mold filling is completed,.

In other words ***"pouring time* or *filling time should be less than the time at which solidification starts".***

Mathematically,

$$\tau_f \le \tau_f^* \qquad (4.2)$$

where τ_f^* = Time elapsed between pouring temperature to start of solidification temperature

τ_f = filling time

The total time to fill the mold cavity can be determined by integrating the incremental time of filling for all layers from bottom to the top of the mold cavity [7].

$$\tau_f = \int_0^{h_m} \left(\frac{A_i}{\sum_{j=1}^{N} A_{ingate\_j} \times V_{ingate\_j}} \right) dh \qquad (4.3)$$

Where A_i = instantaneous cross sectional area of casting layer being filled,

A_{ingate} = cross sectional area of ingate,

V_{ingate} = velocity of molten meal at ingate,

N = number of ingates

The above equation cannot predict other phenomenon in mold filling such as splashing, branching and rejoining of streams.

Substituting equation 4.3 in 4.2, we have

$$\Rightarrow \int_0^{h_m} \left(\frac{A_i}{\sum_{j=1}^{N} V_{ingate\_j} \times A_{g\_j}} \right) dh \le \tau_f^*$$

so for single ingate the expression reduces to :

$$\Rightarrow \int_0^{h_m} \left(\frac{A_i}{V_{ingate} \times A_g} \right) dh \le \tau_f^*$$

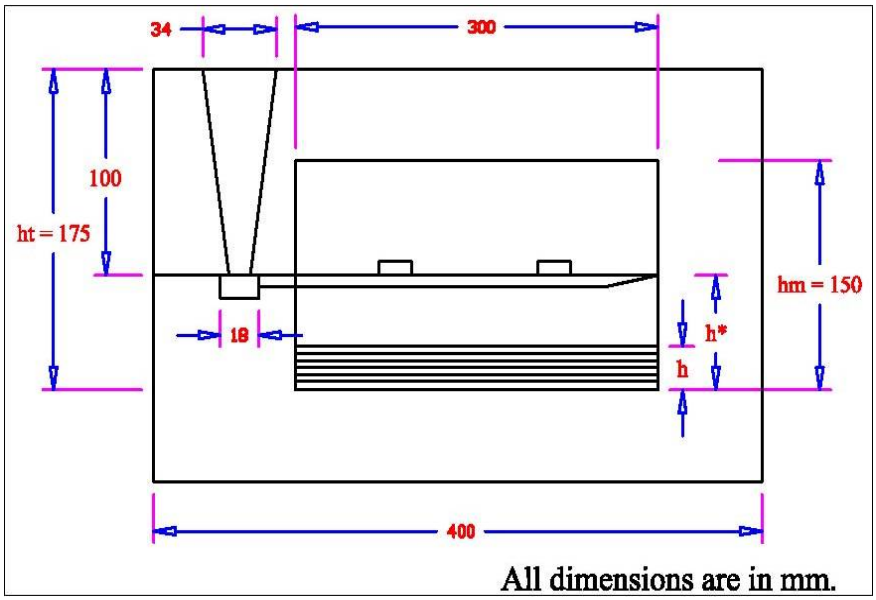

Figure 4.3 Geometric representation of gating system for plate casting

$$\Rightarrow \int_0^{h_m} \left(\frac{A_i}{\sqrt{2 \times g \times (h_t - h)} \times A_g} \right) dh \le \tau_f^* \qquad \left[\because V_{ingate} = \sqrt{2 \times g \times (h_t - h)} \ \ldots \text{ figure 4.3} \right]$$

Where h_t = height between bottom of mold cavity to the top of the mold
and h = instantaneous height of molten metal in the mold cavity

$$\Rightarrow \left(\frac{A_i}{\sqrt{2 \times g} \times A_g} \right) \times \int_0^{h_m} \left(\frac{1}{\sqrt{h_t - h}} \right) dh \le \tau_f^*$$

substituting $\left(\frac{A_i}{\sqrt{2 \times g} \times A_g} \right)$ = constant = C in the above equation we have

$$\Rightarrow C \times \int_0^{h_m} \left(\frac{1}{\sqrt{h_t - h}} \right) dh \le \tau_f^*$$

Take $h = h_t \bullet \cos^2 \theta$

$$\Rightarrow dh = h_t \bullet 2 \cos \theta (-\sin \theta) \bullet d\theta$$

$$\Rightarrow dh = -\sin 2\theta \bullet h_t \bullet d\theta$$

As $h = 0 \quad \Rightarrow \quad \theta = 90;$

$h = h_m \quad \Rightarrow \quad \theta = \cos^{-1} \sqrt{\frac{h_m}{h_t}}$

Changing the limits of integration to θ

$$\Rightarrow C\times \int_{\theta=90}^{\cos^{-1}\sqrt{h_m/h_t}} \left(\frac{-\sin 2\theta \bullet h_t}{\sqrt{h_t - h_t \bullet \cos^2\theta}}\right) d\theta \le \tau_f^*$$

$$\Rightarrow C\times \int_{\cos^{-1}\sqrt{h_m/h_t}}^{90} \left(\frac{\sqrt{h_t}\bullet \sin 2\theta}{\sqrt{1-\cos^2\theta}}\right) d\theta \le \tau_f^*$$

$$\Rightarrow C\times \sqrt{h_t}\times \int_{\cos^{-1}\sqrt{h_m/h_t}}^{90} \left(\frac{\sin 2\theta}{\sin\theta}\right) d\theta \le \tau_f^*$$

$$\Rightarrow C\times \sqrt{h_t}\times \int_{\cos^{-1}\sqrt{h_m/h_t}}^{90} \left(2\bullet\cos\theta\right) d\theta \le \tau_f^*$$

$$\Rightarrow C\times \sqrt{h_t}\times \int_{\cos^{-1}\sqrt{h_m/h_t}}^{90} \left(2\bullet\cos\theta\right) d\theta \le \tau_f^*$$

$$\Rightarrow 2\times C\times \sqrt{h_t}\times \left[\sin\theta\right]_{\cos^{-1}\sqrt{h_m/h_t}}^{90} \le \tau_f^*$$

$$\Rightarrow 2\times C\times \sqrt{h_t}\times \left[\sin 90 - \sin\left(\cos^{-1}\sqrt{h_m/h_t}\right)\right] \le \tau_f^*$$

$$\Rightarrow 2\times C\times \sqrt{h_t}\times \left[1 - \sin\left(\cos^{-1}\sqrt{h_m/h_t}\right)\right] \le \tau_f^*$$

$$\Rightarrow 2\times C\times \sqrt{h_t}\times \left[1 - \left\{1-\left(\cos^2\left(\cos^{-1}\sqrt{h_m/h_t}\right)\right)\right\}^{1/2}\right] \le \tau_f^*$$

$$\Rightarrow 2\times C\times \sqrt{h_t}\times \left[1 - \left\{1-\left(\sqrt{h_m/h_t}\right)^2\right\}^{1/2}\right] \le \tau_f^*$$

$$\Rightarrow 2\times C\times \sqrt{h_t}\times \left[1 - \left\{1-\left(h_m/h_t\right)\right\}^{1/2}\right] \le \tau_f^*$$

Finally, we get

$$C\times 2\left[\sqrt{h_t} - \sqrt{h_t - h_m}\right] \le \tau_f^*$$

Substituting the value of C, we get

$$\sqrt{\frac{2}{g}}\times \frac{A_i}{A_g}\times \left[\sqrt{h_t} - \sqrt{h_t - h_m}\right] \le \tau_f^* \qquad (4.4)$$

From the above equation, as the value of h_t increases the function $f = \sqrt{h_t} - \sqrt{h_t - h_m}$ decreases. Therefore we can say that as the head increases the ingate area requirement reduces.

Let us take an example of 300 x 250 x 150 mm^3 **plate casting** as shown in the figure 4.3

The other dimensions relating to gating system are also indicated in for simplicity. From equation 4.3, it is clear that all other dimensions are constants for a given casting geometry so only variable is ingate area A_g.

For the given example as shown in the figure 4.3

$h_t = 175\ mm = 0.175\ m$
$h_m = 150\ mm\ =\ 0.15\ m$
$h\ =$ instantaneous height of molten metal in the mold cavity
$=\ 5\ mm\ = 0.005\ mm$
$A_i =$ instantaneous cross sectional area of the mold cavity
$= 300\ \times\ 250\ mm^2\ =\ 0.075\ m^2$
$\tau_f^*\ =\ 15$ sec

Substituting these values in equation 4.3 we have

$$\Rightarrow \sqrt{\frac{2}{9.81}} \times \frac{0.075}{A_g} \times \left[\sqrt{0.175} - \sqrt{0.175 - 0.15}\right] \leq 15$$
$$\Rightarrow A_g \geq 5.8746 \times 10^{-4}\ m^2$$
$$\Rightarrow A_g \geq 587.46\ mm^2 \qquad (4.5)$$

From equations 4.4 and 4.5, it is clear that this constraint gives minimal area requirement for the ingate section.

4.2 Constraint 2 (Modulus of Ingate with respect to Connected Section)

Modulus of the ingate should be less than the modulus of the connected section. Mathematically,

$$M_{ingate} \leq M_{conne\_\sec}$$
$$\Rightarrow \left[\frac{\text{volume of ingate}}{\text{cooling surface area of ingate}}\right] \leq \left[\frac{\text{volume of connected section}}{\text{cooling surface area of connected section}}\right]$$
$$\Rightarrow \left[\frac{A_g \times l}{P_g \times l}\right] \leq \left[\frac{V}{A}\right]_{connected\ \text{section}}$$

where l = length of ingate

P_g = perimeter of ingate section

$$\Rightarrow \left[\frac{A_g}{P_g}\right] \leq \left[\frac{V}{A}\right]_{connected\ section} \tag{4.6}$$

For simplicity let's take square section of the ingate as shown in the figure 4.4

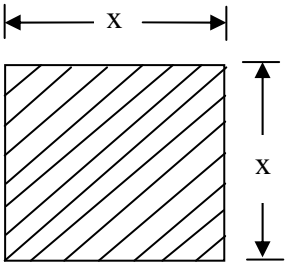

Figure 4.4 Ingate cross sectional area

In our case

$$V = 0.300 \times 0.250 \times 0.150 = 0.01125\ m^3$$
$$A = 2 \times (0.3 \times 0.25 + 0.25 \times 0.15 + 0.15 \times 0.3) = 0.3150\ m^2$$

As shown in figure 4.4

$$A_g = x^2$$
$$P_g = 4 \times x$$
$$\Rightarrow P_g = 4 \times \sqrt{A_g} \tag{4.7}$$

Substituting equation 4.6 in 4.5, we have

$$A_g \leq 0.02041\ m^2 \tag{4.8}$$

From the equation 4.8, it is clear that this constraint gives maximum limit of ingate area.

4.3 Constraint 3 (Mold Erosion)

In case of top and parting line gate, the jet of molten metal attains increment in velocity as it leaves the ingate and strikes the mold-cavity bottom surface. If velocity of impingement exceeds a critical value, it results in mold erosion. Due to this, we have a sand inclusion defect in the final casting.

This can be avoided by using bottom gating system, but it increases the filling time for a given casting as compared to top and parting line gating system. So it does not satisfy our objective function (maximize filling rate).

So for a given sprue height or head to avoid mold erosion problem, the force exerted by the impinging metal stream should be less than the mold strength.

If we resolve the force exerted by metal stream, parallel and perpendicular to the mold bottom surface we get two forces (1) tangential force and (2) normal force. Tangential force induces shear stress in the mold material and normal force induces the compressive stress in the mold material. So we can define the constraint on mold erosion as follows:

(a) "Shear stress induced by melt jet should be less than the shear strength of the mold material."

(b) "Compressive stress induced by the melt jet should be less than compressive strength of the mold material."

Derivation of forces exerted by the melt jet

According to the Newton's second law

Force $F =$ rate of change of momentum

$$= \left(\frac{\text{mass} \times \text{change in velocity}}{\text{time}} \right)$$

$= \dot{m} \times$ change in velocity where $\dot{m}$ = mass flow rate in kg/sec

$= \dot{m} \times \left(\text{final velocity - initial velocity}\right)$

So, for the molten metal striking the bottom of the mold
force exerted by jet on the mold bottom surface = mass flow rate × change in velocity

$$\Rightarrow F = \dot{m} \times \begin{pmatrix} \text{Velocity just before impingement of melt jet} \\ \text{- Velocity just at the time of impingement of melt jet} \end{pmatrix}$$

$$\Rightarrow F = \dot{m} \times \left(V_{impinge} - 0 \right)$$

$$\Rightarrow F = \rho_m \times Q \times V_{impinge}$$

where $V_{impinge}$ = resultant impingement velocity of melt-jet at the mold bottom surface

Q = volume flow rate of molten metal

ρ_m = density of moltem metal

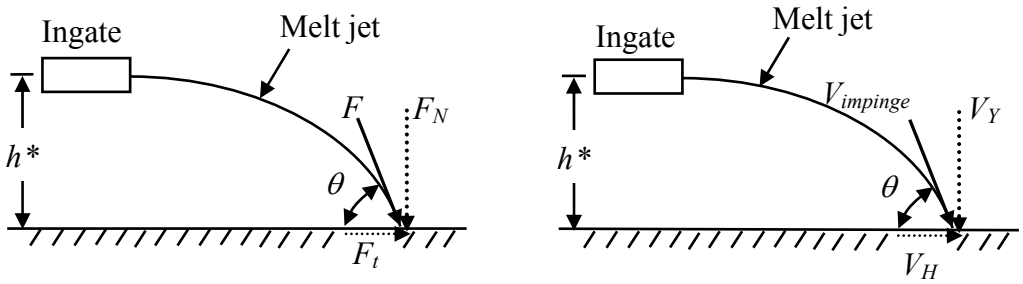

Figure 4.5 (a) Representation of resolved forces of melt jet and (b) Representation of resolved impingement velocity of melt jet

Normal force exerted by the melt-jet

Normal force $F_N = F\sin\theta$ (F = resultant force exerted by melt jet)

$\Rightarrow F_N = \rho_m \times Q \times V_{impinge}\sin\theta$

$\Rightarrow F_N = \rho_m \times \left(A_g \times V_g\right) \times V_{impinge}\sin\theta$ $\left(\because \text{Q} = A_g \times V_g = \text{Volume flow rate of molten metal}\right)$

Assuming that melt jet area at the point of impingement is same as melt jet area at ingate

$\Rightarrow A_{impinge} = A_g$

After substutuing this value in the previous equation, we have

$\Rightarrow F_N = \rho_m \times \left(A_{impinge} \times V_g\right) \times V_{impinge}\sin\theta$

$\Rightarrow \dfrac{F_N}{A_{impinge}} = \rho_m \times V_g \times V_{impinge}\sin\theta$

$\Rightarrow \sigma_Y = \rho_m \times V_g \times V_{impinge}\sin\theta$ $\left(\because \dfrac{F_N}{A_{impinge}} = \text{induced compressive stress} = \sigma_Y\right)$

$\Rightarrow \sigma_Y = \rho_m \times V_g \times V_Y$ $\left(\because V_Y = \text{vertical component of impingement velocity} = V_{impinge}\sin\theta\right)$

$\Rightarrow \sigma_Y = \rho_m \times V_g \times \left(V_{Y0} + a_Y \times t_{flight}\right)$ $\left(V_{Y0} = \text{initial vertical component of velocity}\right)$

For projectile motion $a_Y = -\text{g}$

$\Rightarrow \sigma_Y = \rho_m \times V_g \times \left(V_{Y0} - g \times t_{flight}\right)$

$$\Rightarrow \sigma_Y = \rho_m \times V_g \times \left(V_{Y0} - g \times \frac{1}{g}\left[V_{Y0} + \sqrt{V_{Y0}^2 + 2 \times g \times h^*} \right] \right) \quad \text{.....} (4.9)$$

To avoid mold erosion,
compressive stress $\leq$ compressive strength of mold

$$\Rightarrow \sigma_Y \leq S_Y \quad (4.10)$$

substituting equation 4.10 in 4.9, we get

$$\Rightarrow \rho_m \times V_g \times \left(\sqrt{V_{Y0}^2 + 2 \times g \times h^*} \right) \leq S_Y$$

In the case of parting line or top gating system, we have
Initial projection angle, $\theta = 0$

$$\text{As } \theta = 0 \Rightarrow V_{Y0} = V_g \sin\theta = 0$$

From the figure 4.3 , $h^* = h_t - 0.1$
substituting the value of V_{Y0} and h^* in the equation 4.10, we have

$$\Rightarrow \sigma_Y = \rho_m \times V_g \times \left(0 - g \times \frac{1}{g}\left[0 + \sqrt{0 + 2 \times g \times (h_t - 0.1)} \right] \right)$$

$$\Rightarrow \sigma_Y = \rho_m \times V_g \times \sqrt{2 \times g \times (h_t - 0.1)} \text{ .... } (compressive) \quad (4.11)$$

Now compressive stress induced by the melt jet should be less than compressive strength of the mold material.

That is,

$$\sigma_Y \leq S_Y \quad (4.12)$$

Substituting equation 4.11 in 4.12, we have

$$\rho_m \times V_g \times \sqrt{2 \times g \times (h_t - 0.1)} \leq S_Y \quad (4.13)$$

For aluminium
S_Y = mold compressive strength =117.19 kPa [8]
S_H = mold shear strength = 68.94 kPa [8]

Substituting these values in equation 4.13, we have

$$2380 \times V_g \times \sqrt{2 \times 9.81 \times (0.175 - 0.1)} \leq 117198$$
$$\Rightarrow V_g \leq 40.59 \ m/\sec \qquad (4.14)$$

Tangential force exerted by the melt-jet

$$\begin{aligned} F_T &= F\cos\theta \\ &= \rho_m \times Q \times V_{impinge} \times \cos\theta \\ &= \rho_m \times \left(A_g \times V_g\right) \times V_{impinge} \times \cos\theta \end{aligned}$$

substituting $A_{impinge} = A_g$, we get

$$F_T = \rho_m \times A_{impinge} \times V_g \times V_{impinge} \times \cos\theta$$
$$\Rightarrow \frac{F_T}{A_{impinge}} = \rho_m \times V_g \times V_{impinge} \times \cos\theta \qquad \left(\frac{F_T}{A_{impinge}} = induced\ compressive\ stress = \sigma_H\right)$$
$$\Rightarrow \sigma_H = \rho_m \times V_g \times V_{impinge} \times \cos\theta$$

As we know during projectile motion, horizontal component of velocity remains constant only vertical component of velocity changes.

Hence $V_H = V_g = V_{impinge} \times \cos\theta$
$\Rightarrow \sigma_H = \rho_m \times V_g \times V_g$
$\Rightarrow \sigma_H = \rho_m \times V_g^{\,2}$

To avoid mold erosion ,
Shear stress $\leq$ Shear strength of mold

$$\Rightarrow \sigma_H \leq S_H$$
$$\Rightarrow \rho_m \times V_g^{\,2} \leq S_H \qquad (4.15)$$
$$\Rightarrow 2380 \times V_g^2 \leq 68.94 \times 10^3$$
$$\Rightarrow V_g \leq 5.382 \ m/\sec$$

From equations 4.14 and 4.15, it is clear that this constraint gives maximum limit of velocity of molten metal at the ingate. Beyond that velocity mold erosion takes place.

4.4 Constraint 4 (Reynolds Number)

Molten metal flows through the gating system to the mold cavity. Due to complexity of mold cavity it is not possible to get laminar flow in the mold cavity. It is either turbulent or semi turbulent flow. Low Reynolds number reduces the casting yield because it increases the dimensions of sprue, runner and ingates. Conversely high Reynolds number leads to turbulent flow. So in order to avoid highly turbulent flow, Reynolds number should be less than 20000, which results in semi-turbulent flow [35].

$\mathrm{Re} \le 20000$ ..... semi turbulent flow

$$\Rightarrow \frac{\rho_m \times V_g \times d}{\mu_m} \le 20000 \qquad (\mu_m = \text{ dynamic viscocity of molten metal})$$

$$\Rightarrow V_g \times d - \frac{\mu_m}{\rho_m} \times 20000 \le 0 \qquad (4.16)$$

$$d \text{ = characteristic length } = 4 \times \frac{\text{cross sectional area}}{\text{wetted perimeter}} \quad \text{(for non-circular section)}$$

$$= \frac{4 \times A_g}{P_g}$$

From equation 4.6, for square ingate $P_g = 4 \times \sqrt{A_g}$

hence, substituting equation 4.6 in 4.16, we have

$$V_g \times \sqrt{A_g} - \frac{\mu_m}{\rho_m} \times 20000 \le 0 \qquad (4.17)$$

for Aluminium

dynamic viscosity, $\mu_m = 0.012\ N - s / m^2$

and $\rho_m = 2380\ m^2/\mathrm{s}$

hence kinematic viscosity, $\gamma_m = \frac{\mu_m}{\rho_m} = \frac{0.012}{2380} = 5.042 \times 10^{-6}\ m^2/\mathrm{s}$

After substitutintg these values in equation 4.17, we have

$$\Rightarrow V_g \times \sqrt{A_g} - 0.10084 \le 0 \qquad (4.18)$$

4.5 Constraint 5 (Limit of Quick Filling)

From the fluid dynamics study, it is clear that as the molten metal flows into the mold cavity, the molten metal front rises against the gravity. As far as the metallostatic pressure head of the molten metal is greater than the pressure of mold gases above it a positive flow will take place. Whenever the molten metal layer rises into the mold cavity in a layer-by-layer manner, due to change of elevation the metallostatic pressure will decreases and at the same time due to compression of gases along with the generation of new gases at each metal layer the Pressure created by mold gases will increase.

When both equalize at that time no flow condition prevails and an equilibrium condition exist between mold gases and the molten metal flow.

Mathematically,

$$P_{mold\_i} = P_{metallostaic} \text{ ..... No flow condition} \quad (4.19)$$

However if the pressure created by mold gases exceeds the metallostatic pressure exerted by molten metal, a reversal flow situation occurs and results in incomplete filling which is unacceptable.

Mathematically,

$$P_{mold\_i} > P_{metallostaic} \text{ ..... reversal flow condition} \quad (4.20)$$

From equation 4.19 and 4.20, in order to get positive flow, pressure exerted by the mold gases should be less than or equal to metallostatic pressure.

$$\Rightarrow P_{mold\_i} \leq P_{metallostatic} \quad (4.21)$$

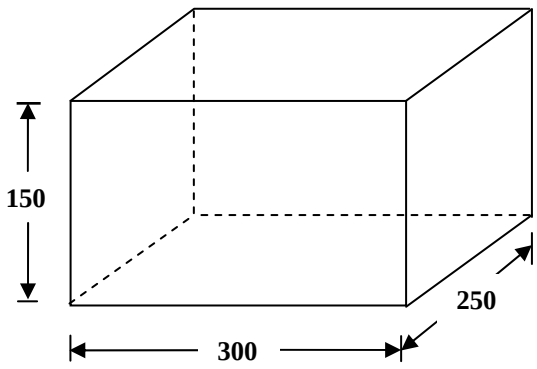

Figure 4.6 plate shaped casting

$A = 300 \times 250 \times 10^{-6} = 0.075\ m^2$

$h_m = 150\ mm = 0.15\ m$

Considering mold cavity is divided in to number of layers

Let us say each layer is having layer thickness $dl = 5\ mm$

Pouring height $= 30\ mm = 0.03\ m$

Take an effective thickness $t_{eff} = 2\ mm$

Mold dimensions

Length $= 400$ mm, Width $= 300$ mm, Height $= 200$ mm

Total sand volume = Mold box volume − Mold cavity volume

$= [400 \times 300 \times 200] - [300 \times 250 \times 150]$

$= 12750000\ mm^3$

$= 0.01275\ m^3$

Thermodynamic properties of mold

$K_{mold} = 0.5\ W / m°K$

$T_{mold} = 353\ W / m°K$

Metal properties for aluminium

$\rho_m = 2700\ kg / m^3$

$T_p = 948\ °K$

$T_m = 823\ °K$ (Meting point temperature)

for layer -1

metallostatic pressure $P_{metallostatic} = \rho_m \times g \times (h_t + \text{pouring height} - h)$

$= 2700 \times 9.81 \times (0.175 + 0.03 - 0.005)$

$= 5297.4\ N / m^2$

volume of metal layer, $V_{Layer\_1} = 300 \times 250 \times dl$

$= 300 \times 250 \times 5 \times 10^{-9}$

$\therefore V_{Layer\_1} = 3.75 \times 10^{-4}\ m^3$

Gas volume $V(1) = 300 \times 250 \times 145 \times 10^{-9}$

$= 0.010875\ m^3$

Let $\tau_1 =$ time taken to fill 1^{st} metal layer up to $dl = 5\ mm$

Let $V_{Layer\_i} =$ volume of metal layer at time instant *i*

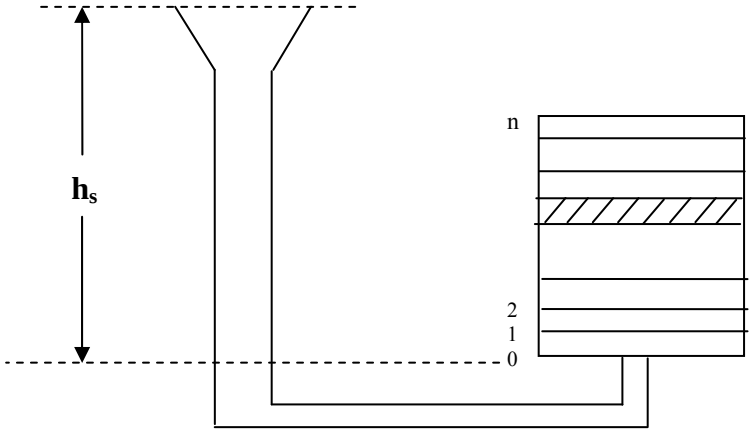

Figure 4.7 Arrangement of gating system for the casting

For i^{th} time instant we have

$$\tau_i = \frac{\text{Volume of metal layer at any time instant } \tau_i}{\text{Volume flow rate of melt in the mold cavity}}$$

$$\Rightarrow \tau_i = \frac{V_{Layer\_i}}{A_g \times V_g}$$

Hence for the 1^{st} layer at any time instant τ_1, we have

$$\tau_1 = \frac{V_{Layer\_1}}{A_g \times V_g} = \frac{3.75 \times 10^{-4}}{A_g \times V_g} \text{ sec}$$

The most common method used to make metal sand castings is green sand molding. In this process, granular refractory sand is coated with a mixture of bentonite clay, water and, in some cases, other additives. The additives help to harden and hold the mold shape to withstand the pressures of the molten metal.

The green sand mixture is compacted through mechanical force or by hand around a pattern to create a mold. The mechanical force needed for the sand casting process can be induced by slinging, jolting, squeezing or by impact/impulse. For many metal applications, green sand casting processes are the most cost-effective of all metal forming operations.

Thus green sand molding is a mixture of silica sand, binder, water and additives. Generally, bentonite is used as a binding agent and Sea coal is used as additive for the facing sand.

The composition of various ingredients is as follows.

Silica sand = 80 to 90%, Clay content (bentonite) = 5 to 20 %, Moisture content = 2 to 8 % and Sea coal = 4-5%

For modeling, taking some values as follows.
Silica sand = 85 %, Bentonite =6%, Moisture content = 4 % and Sea coal =5%

In India majority of coal available is of bituminous type. So taking sea coal is of bituminous type. From the fuels and combustion by Prof. Samir Sarkar [36], we have

The composition of bituminous coal available in India obtained by ultimate analysis of coal samples from various places in India has following ingredients in different ranges.

Carbon - 80 to 90 %, Oxygen - 0.5 to 15 %, Hydrogen - 1 to 6 % and Nitrogen - 1 to 10 %

The above values of composition may differ slightly for the coals of other countries.
For modeling purpose, let's take some values of composition.

Carbon - 85 %, Oxygen - 7 %, Hydrogen - 1 % and Nitrogen - 7 %

$$\begin{aligned}\text{Total sand weight} &= \rho_{sand} \times \text{sand volume} \\ &= 1600 \times 0.01275 \\ &= 20.4\ kg\end{aligned}$$

Now Sea coal volume = 5% of molding sand volume
So for effective layer thickness $of\ t_{eff} = 2\ mm$

$$\begin{aligned}\text{Sea coal volume} &= 5\%\ of \begin{bmatrix}\text{outer volume up to } t_{eff} \text{ for the } 1^{st} \text{ layer} \\ -\ \text{inner box volume of } 1^{st} \text{ layer}\end{bmatrix} \\ &= 0.05 \times \left[(304 \times 254 \times 7) - (300 \times 250 \times 5)\right] \times 10^{-9} \\ &= 8.2756 \times 10^{-6}\ m^3 = 8.2756\ cc\end{aligned}$$

$$\begin{aligned}\text{Sea coal weight} &= \rho_{sea-coal} \times \text{Sea coal volume} \\ &= 0.56 \times 8.2756 \qquad (\because \rho_{sea-coal} = 0.56 \text{ gram/cc}) \\ &= 4.6343 \text{ grams}\end{aligned}$$

$$\begin{aligned}\text{Now} \quad \%\ C &= 85\% \text{ of total weight} \\ &= 0.85 \times 4.6353 = 3.9391 \text{ grams} \\ \text{Similarly } \%\ H_2 &= 1\% \text{ of total weight} \\ &= 0.01 \times 4.6353 = 0.04635 \text{ grams}\end{aligned}$$

$\% N_2 =$ 7% of total weight

$= 0.07 \times 4.6353 = 0.3245$ grams

$\% O_2 =$ 7% of total weight

$= 0.07 \times 4.6353 = 0.3245$ grams

During filling chemical reaction will take place and the carbon present in sea coal react with oxygen present in the mold cavity to form CO_2.

$$C + O_2 \overset{\Delta}{\rightleftharpoons} CO_2$$

$$\Rightarrow 12.011 \; grams \; of \; \text{C} \xrightarrow{\text{Produces}} 43.991 \; grams \; of \; CO_2$$

$$\Rightarrow 3.9391 \; grams \; of \; \text{C} = ?$$

$$= 3.9391 \times \frac{43.991}{12.011} = 14.4271 \; grams \; CO_2 \text{ emission}$$

According to *Dalton's law of partial pressure* the total pressure exerted by the gaseous mixture is equal to the sum of partial pressures exerted by the individual gas component when occupies same volume as that of the volume of gas mixture at the same temperature.

Applying this law to the our case, we have

$$P_{mold\_i} = P_{additive\_gases} + P_{moisture\_gases} + P_{binder\_gases} + \Delta P_{air\_i} - P_{gas\_per\_i}$$

where,

$$P_{additive\_gases} = P_{CO_2} + P_{O_2} + P_{N_2} + P_{H_2}$$

$$P_{moisture\_gases} = P_{O_2} + P_{H_2}$$

calculating partial pressures of these gases:

$$P_{CO_2} = \frac{\eta_{CO_2} \times R_{CO_2} \times T}{V}$$

where η_{CO_2} = Total number of moles of CO_2 present in the mixture of gases

$$\eta_{CO_2} = \frac{m}{M} = \frac{\text{total mass}}{\text{molar mass}} = \frac{14.4271}{43.991} = 0.3279 \; mols$$

$$\text{Now } R_{CO_2} = \frac{8.314}{M_{CO_2}} = \frac{8.314}{43.991} = 0.1889 \; J / gram \; ^{\circ}\text{K}$$

Similarly,

$$R_{O_2} = \frac{8.314}{M_{O_2}} = \frac{8.314}{32.98} = 0.2599\ J/gram\ ^\circ\text{K}$$

$$R_{N_2} = \frac{8.314}{M_{N_2}} = \frac{8.314}{28.01} = 0.2968\ J/gram\ ^\circ\text{K}$$

$$R_{H_2} = \frac{8.314}{M_{H_2}} = \frac{8.314}{2(1.0079)} = 4.1244 J/gram\ ^\circ\text{K}$$

Let us calculate partial pressure of individual gas in a mixture of gases.

$$P_{CO_2} = \frac{\eta_{CO_2} \times R_{CO_2} \times T_i}{V(1)} = \frac{0.3279 \times 0.1889 \times 948}{0.010875} = 5400.43 N/m^2$$

Now calculating number of moles of H_2, O_2 and N_2 present in the mould cavity

$$\eta_{O_2} = \frac{\text{total weight of } O_2}{\text{molecular weight of } O_2} = \frac{0.3245}{31.98} = 0.01014\ moles$$

$$\eta_{H_2} = \frac{\text{total weight of } H_2}{\text{molecular weight of } H_2} = \frac{0.04635}{2.0158} = 0.02299\ moles$$

$$\eta_{N_2} = \frac{\text{total weight of } N_2}{\text{molecular weight of } N_2} = \frac{0.3245}{28.01} = 0.01158\ moles$$

Partial pressures exerted by these gases are

$$P_{O_2} = \frac{\eta_{O_2} \times R_{O_2} \times T_i}{V(1)} = \frac{0.01014 \times 0.2599 \times 948}{0.010875} = 229.73 N/m^2$$

$$P_{H_2} = \frac{\eta_{H_2} \times R_{H_2} \times T_i}{V(1)} = \frac{0.02299 \times 4.1244 \times 948}{0.010875} = 8264.882 N/m^2$$

$$P_{N_2} = \frac{\eta_{O_2} \times R_{O_2} \times T_i}{V(1)} = \frac{0.01158 \times 0.2968 \times 948}{0.010875} = 299.68\ N/m^2$$

Moisture Gases:

Moisture Properties

$$\rho_{H_2O}(at\ 1\ bar\ and\ 300^\circ K) = 1000\ kg/m^3$$

$$R_{H_2O} = 287\ J/kg\ ^\circ K$$

As we know when moisture in the molding sand comes in contact with hot molten metal it absorbs heat from the melt and decomposes hydrogen and nitrogen gases. The chemical equation representing this phenomenon is as follows.

$$H_2O \overset{\Delta}{\rightleftharpoons} H_2 + \frac{1}{2}O_2$$

$$\Rightarrow 18\ grams\ \text{of}\ H_2O \xrightarrow{Produces} 2\ grams\ \text{of}\ H_2 + 16\ grams\ \text{of}\ O_2$$

Calculating the volume of water present in the moulding sand upto to an effective *t*hickness of 2 *mm* from the mold walls

V_{H_2O} = 4% of total volume

= 0.04 (outer volume - inner volume)

$$\Rightarrow V_{H_2O} = 0.04\ \left[(304\times254\times7) - (300\times250\times5)\right]\times10^{-9}$$

$$= 6.6204\times10^{-6}\ m^3$$

Mass of H_2O present $= \rho_{H_2O}\times V_{H_2O}$

$$\Rightarrow m_{H_2O} = 1000\times6.6204\times10^{-6} = 6.6204\times10^{-3}m^3$$

$$\Rightarrow m_{H_2O} = 6.6204\ grams$$

From the chemical equation we have

$$18\ grams\ of\ H_2O \xrightarrow{Produces} 2\ grams\ of\ H_2$$

$$\Rightarrow\ 6.6204\ grams\ of\ H_2O \xrightarrow{Produces} ?$$

$$\Rightarrow m_{H_2} = \frac{6.6204\times2.0158}{18} = 0.7414\ grams = 0.7414\times10^{-3}\ kg$$

Similarly,

$$18\ grams\ of\ H_2O \xrightarrow{Produces} 16\ grams\ of\ O_2$$

$$\Rightarrow\ 6.6204\ grams\ of\ H_2O \xrightarrow{Produces} ?$$

$$\Rightarrow m_{O_2} = \frac{6.6204\times16}{18} = 5.8848\ grams = 5.8848\times10^{-3}\ kg$$

Calculating number of mols of H_2 and O_2 gas in the mold cavity

$$\eta_{H_2} = \frac{Total\ weight\ of\ H_2}{Molecular\ weight\ of\ H_2} = \frac{0.7414}{2.0158} = 0.3677\ moles$$

$$\eta_{O_2} = \frac{Total\ weight\ of\ O_2}{Molecular\ weight\ of\ O_2} = \frac{5.8848}{31.98} = 0.1840\ moles$$

Partial pressure exerted by H_2 and O_2 gas is given by

$$P_{H_2} = \frac{\eta_{H_2}\times R_{H_2}\times T_i}{V(1)} = \frac{0.3677\times4.1244\times10^{-3}\times948}{0.010875} = 132.20N/m^2$$

$$P_{O_2} = \frac{\eta_{O_2}\times R_{O_2}\times T_i}{V(1)} = \frac{0.1840\times0.2599\times948}{0.010875} = 4168.72\ N/m^2$$

Increase in air pressure

$$m_{air}(1) = \frac{P_{air}(0) \times V(0)}{R_{air} \times T_{air}}$$

where $V(0) = 300 \times 250 \times 150 \times 10^{-9}\ m^3 = 0.01125\ m^3$

$$m_{air}(1) = \frac{1.01325 \times 10^5 \times 0.01125}{287 \times 948} = 4.189 \times 10^{-3}\ kg$$

$$P_{air}(1) = \frac{m_{air}(1) \times R_{air} \times T_i}{V(1)} = \frac{4.189 \times 10^{-3} \times 287 \times 948}{0.010875} = 104818.96\ \text{N} / m^2 (abs)$$

In the sand casting due to permeability of the sand mold the gases escape through the pores of the sand mold, hence pressure of the mold gases will reduce. Now from the standard permeability equation we have,

$$P_{gas\_per\_i} = \frac{V(1) \times t_{mold}}{V_{sand} \times f \times \tau_i}$$

where f = sand permeability number = 90

$$P_{gas\_per\_i} = \frac{0.010875 \times 0.025}{0.01275 \times 90 \times \left(\frac{3.75 \times 10^{-4}}{A_g \times V_g} \right)} = 0.63181 \times A_g \times V_g\ N / m^2$$

$$\begin{aligned} P_{gas\_i} &= P_{moisture\_gases} + P_{additive\_gases} + P_{binder\_gases} \\ &= \left(P_{O_2} + P_{H_2} \right) + \left(P_{CO_2} + P_{O_2} + P_{N_2} + P_{H_2} \right) \\ &= \left(4168.72 + 132.20 \right) + \left(5400.43 + 229.73 + 299.68 + 8264.882 \right) \\ &= 18495.64\ N / m^2 \end{aligned}$$

$$\begin{aligned} P_{mold\_i} &= P_{gas\_i} + \Delta P_{air\_i} - P_{gas\_per\_i} \\ &= P_{gas\_i} + P_{air}(1) - P_{air}(0) - P_{gas\_per\_i} \\ &= 18495.64 + 104818.96 - 101325 - 0.63181 \times A_g \times V_g \\ &= 21989.6 - 0.63181 \times A_g \times V_g \end{aligned} \qquad (4.22)$$

$$\begin{aligned} P_{metallostatic} &= \rho_m \times g \times h_t \\ &= 5297.4\ N / m^2 \end{aligned} \qquad (4.23)$$

Substituting equations 4.22 and 4.23 in 4.21, we get

$$\Rightarrow 21989.6 - 0.63181 \times A_g \times V_g \le 5297.4$$

$$\Rightarrow 16692.2 - 0.63181 \times A_g \times V_g \le 0 \qquad (4.24)$$

The objective function and formulated constraints are then implemented in the SQP optimization algorithms, that are described in the next chapter.

Chapter 5

Results and Discussions

The methodology developed for the optimization in this project has been tested by taking an example of plate casting. The case study is carried out for a plate casting having dimensions of 300 x250 x150 mm. The example demonstrates the optimization of filling rate by considering constraints mentioned in the chapter 4. The optimized value of design constraints (area and velocity of ingate) is then used to find out final gating dimensions based on a gating ratio selected.

5.1 Case study – Plate Casting

This section demonstrates step by step procedure of optimization starting from the constraints formulation, then after optimization using SQP algorithm and finally evaluating the dimensions of the gating channels. The SQP algorithm is given in appendix I and source code to get the dimensions of gating system is given in the appendix II. The various steps to optimize the fill rate of molten metal in the casting cavity is presented in the following flow chart. The various steps are described in figure 5.1 in a step by step manner for a plate casting.

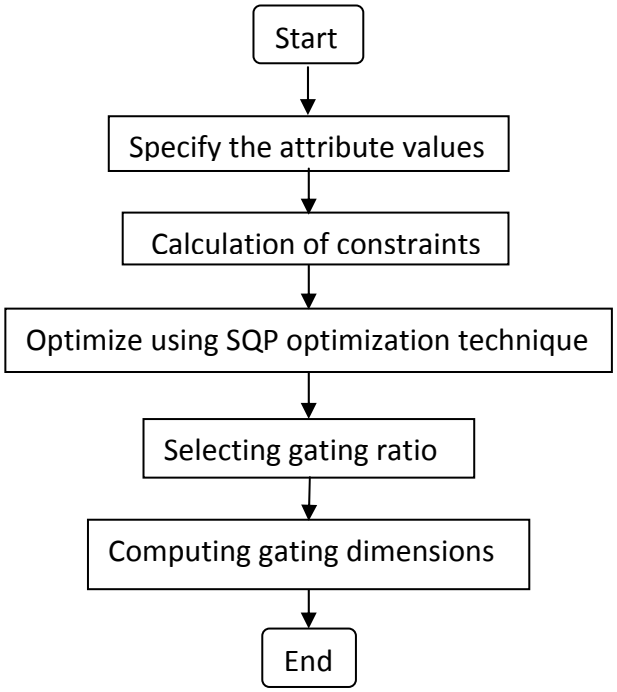

Figure 5.1 Flow chart to maximize filling rate of molten metal in the casting cavity

Step I: Specifying the Attribute Values

This step involves the input to be given for the process. To initialize optimization process, the casting geometry related dimensions are given as input. The other inputs like material, mold and binder properties are tabulated in the table 5.1.

Table 5.1 Input for the process

Attribute	**Value**
Casting dimensions	300 x 250 x 150 mm
Material	Aluminum grade 6061
Minimum mold thickness	20 mm
Pouring to solidification time	15 sec
Minimum layer thickness	5 mm
Liquid density of metal	2380 kg/m^3
Dynamic viscosity of metal	0.012 N-s/m^2
Pouring height	30 mm
Effective thickness	2 mm
Density of sea coal	5600 kg/m^3
Pouring temperature	948 K
Initial pressure of air in mold cavity	1.013 KPa
Mold compressive strength	117.198 KPa
Sand permeability	90
Gating ratio	1: 2: 1.5

Step II : Calculation of Constraints

This step calculates the various design constraints values based on the mathematical formulation described in the chapter 4. Based on the input attribute values, the design constraints limiting the filling rate are computed by the program as follows.

1. Pouring time constraint : $0.002 - A_g \leq 0$
2. Modulus constraint : $A_g - 0.065 \leq 0$
3. Mold erosion constraint : $V_g - 28.704 \leq 0$
4. Reynolds number constraint : $V_g \times \sqrt{A_g} - 0.1 \leq 0$
5. Quick filling constraint : $16692.2 - 0.632 \times A_g \times V_g \leq 0$

The above formulated constraints depend upon the casting geometry, material to be cast, additive and binder properties, sand permeability etc. These constraints are used as an input to the optimization process. This is illustrated well in step 3 below.

Step III : Optimization of Gating Dimensions

This step optimizes the process parameter (area of ingate and the velocity at the ingate). It can be seen from the process constraints obtained from the previous step, that some process constraints are nonlinear, so it is required to use non-linear optimization technique. Hence in order to optimize the above computed process constraints, an SQP optimization technique is used as it gives fast convergence rate and computational time is also very less than other optimization techniques. To get the optimized values a code for the SQP technique has been generated which is used for evaluation of the parameter. The design constraints computed are fed as input to the optimization code. The output from the SQP is optimized value of the design variable that is, area of ingate and velocity at the ingate. The figure 5.2 shows the 3-D plot of objective function with respect to design variables, area of ingate and velocity of ingate. The contour plot at each level set is also plotted in the figure 5.2.

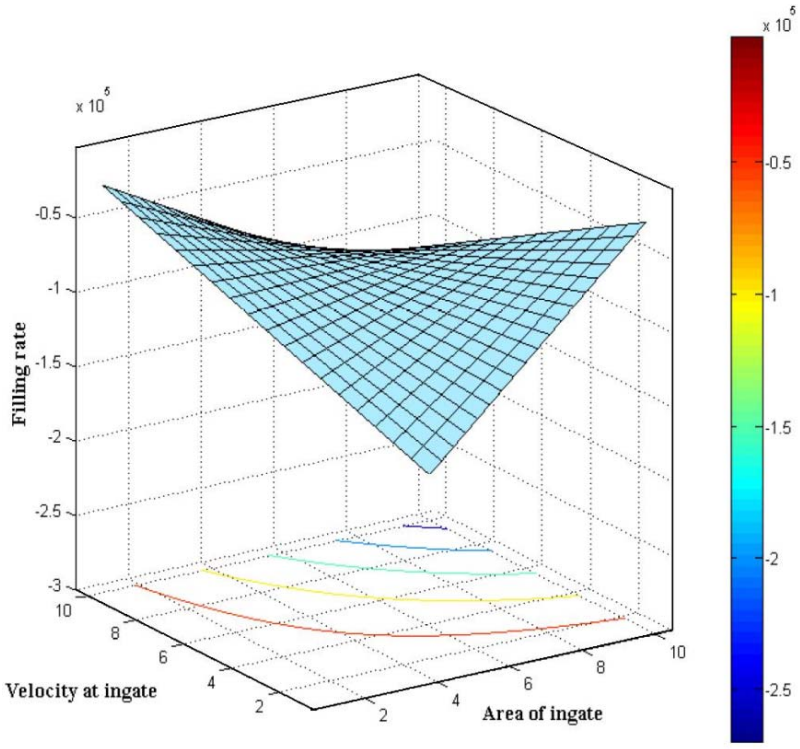

Figure 5.2 3-D plot of design variables Vs filling rate

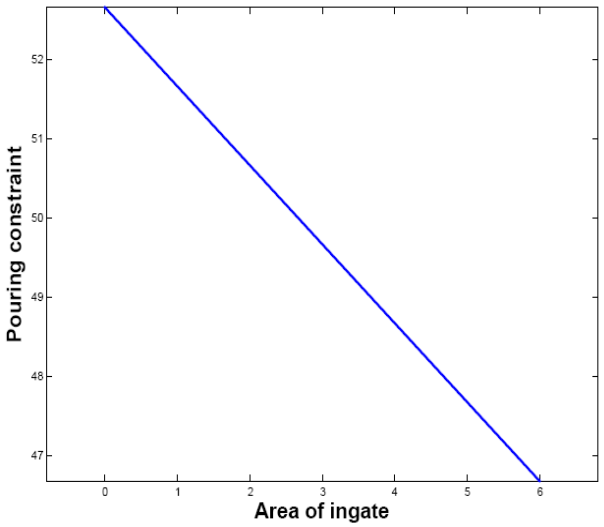

(a) Pouring constraint *Vs* A_g

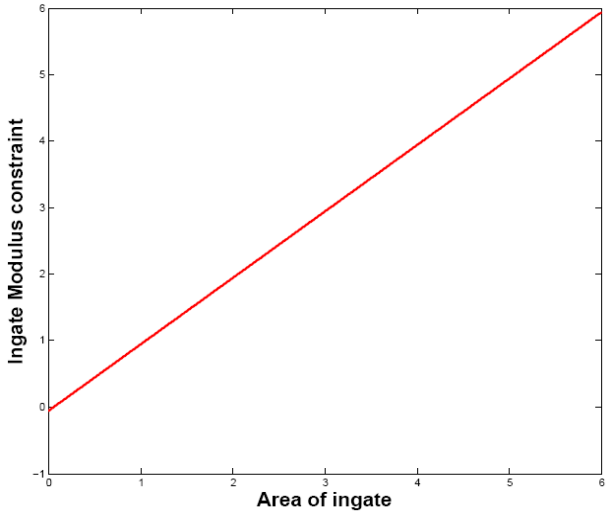

(b) Ingate modulus constraint *Vs* A_g

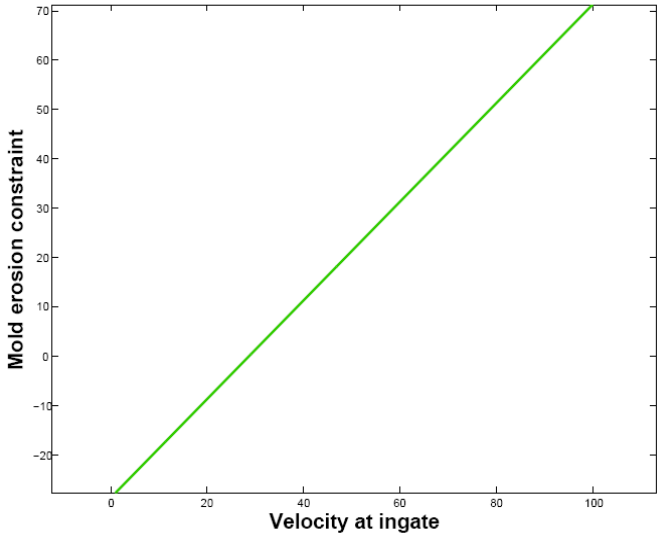

(c) Mold erosion constraint *Vs* V_g

Figure 5.3 Linear variation of design constraints with design parameters

From figure 5.3(a) and (b), it is clear that pouring constraint and ingate modulus constraint varies linearly with the design variable ingate area. Figure 5.3(c) shows that mold erosion constraint varies linearly with ingate velocity of molten metal. However, there are some constraints which vary with both the design variables. It can be viewed from figure 5.4(a) and (b). As shown in figure 5.4(a), Reynolds number varies nonlinearly with design variables A_g and V_g. Similarly we have non linear variation of design parameter A_g and V_g with Quick filling constraint which is shown in figure 5.4(b).

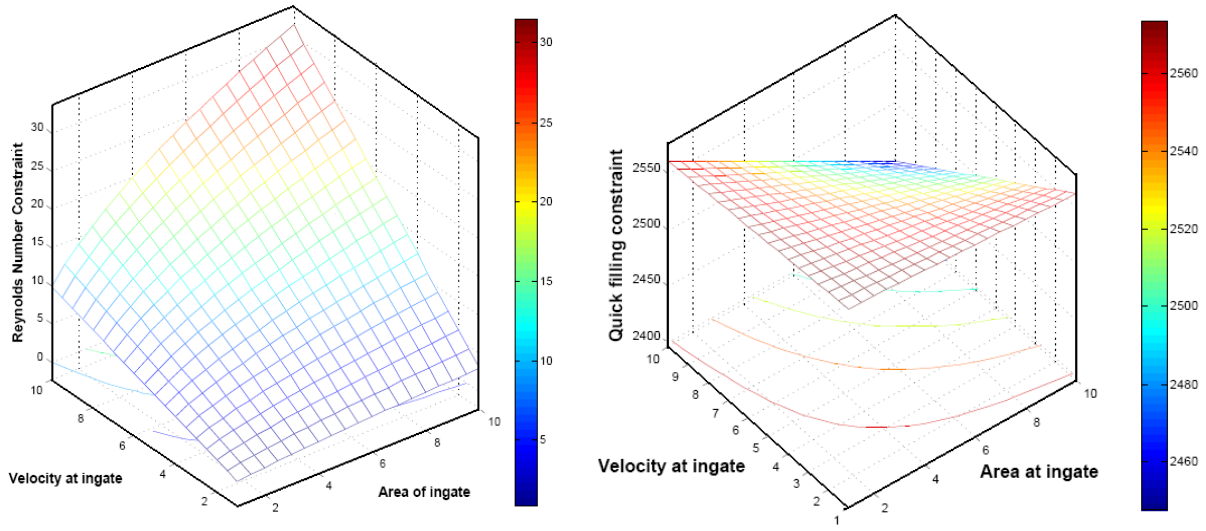

(a) Reynolds number constraint *Vs* A_g & V_g (b) Quick fill constraint *Vs* A_g & V_g

Figure 5.4 Non-linear variation of design constraints with design parameters

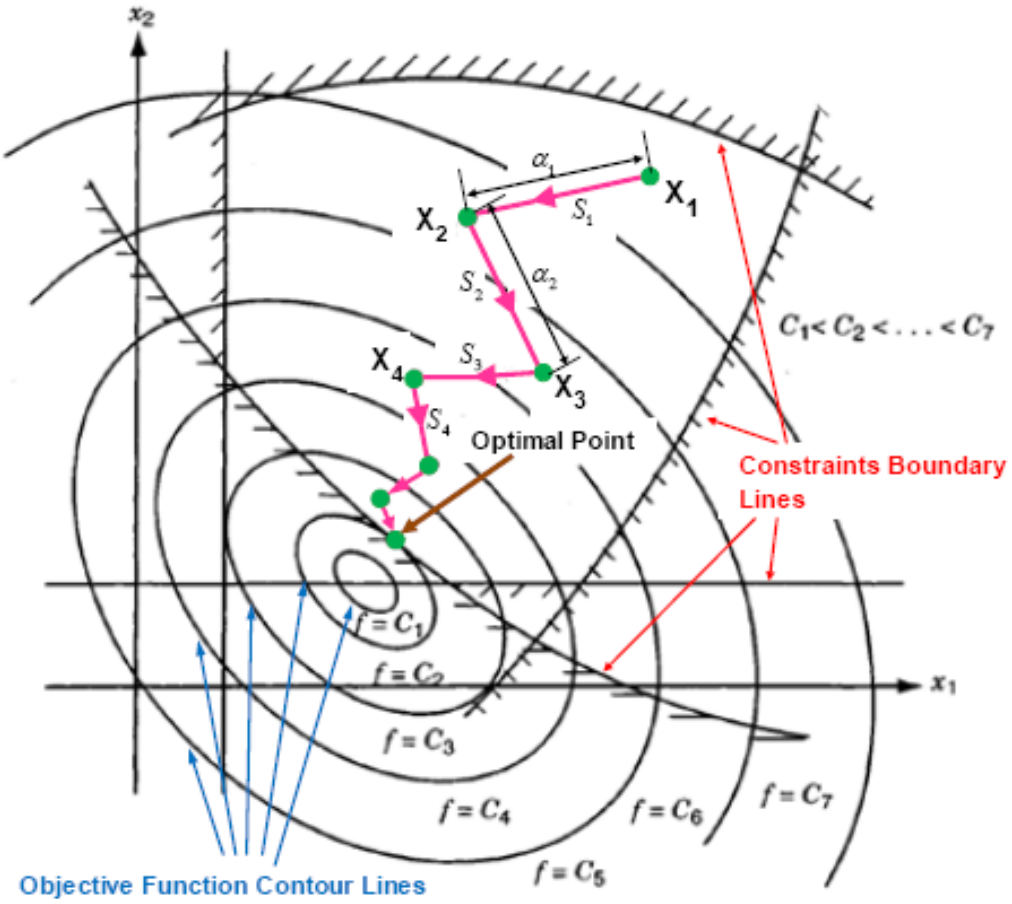

Figure 5.5 Iterative process of optimization

In order to start the optimization process it is required to input initial guess solution as shown in figure 5.5 by vector X_1. From the point algorithm finds the search direction as shown in the figure 5.5 by S_1, which minimizes the objective function. Then after in a given direction S1, algorithm computes the step length α_1 which minimizes the objective function to minimum. From the computed value of S_1 and α_1 the new design vector X_2 can be computed by the algorithm using equation $X_2 = X_1 + \alpha_1 . S_1$ from design point X_2 once again algorithm finds search direction S_2 and calculate step parameter α_2, from which new design vector X_3 is computed. This process continues until optimal solution is reached as shown in figure 5.5. The optimal value of gating dimensions in our case study can be computed as follows by this process.

Iteration number	Area of ingate (m^2)	Velocity at ingate (m^2/sec)
1	0.00583	6.58
2	0.00272	5.36
3	0.00489	3.29
4	0.00135	1.87

Area of ingate $\left(A_g\right) = 0.00135$ m^2 ;
Velocity at the ingate $\left(V_g\right)$ = 1.876 m/sec

For the selected gating ratio of 1:2:1.5, sprue and runner dimensions are listed below.

Area of sprue exit = 0.0009011 m^2 ;
Runner cross sectional area = 0.001800 m^2

Chapter 6

Conclusions

6.1 Summary of Work

A methodology for gating design optimization for sand casting process to maximize the filling rate has been described. It helps to avoid premature freezing in long and thin section castings where molten metal looses heat rapidly, thus it avoids cold shut and misrun related defects in these castings. This methodology increases the production rate of the castings in order to meet the customer order within the due date.

The objective function is to maximize the filling rate of molten metal at the ingate $\left(\rho \times A_g \times V_g\right)$.The design constraints which limit the filling process have been formulated. The various design constraints used are pouring time of molten metal, modulus of ingate with respect to the connected section, mold erosion constraint, Reynolds number and limit on quick filling. All these constraints are presented in the form of two design variables namely area of ingate and the velocity of molten metal at ingate. For most of the metals the variation in the liquid density above the melting point temperature is very small, hence for the analysis it is taken as constant.

As the convergence rate of the SQP technique is very fast, it is used for optimizing the filling rate of molten metal in to the casting cavity along with satisfying the aforementioned design constraints. A programming for SQP algorithm with formulated constraints is carried out to achieve this task. The developed methodology is then implemented for a plate casting to get gating dimensions for maximum filling rate.

6.2 Future Scope

The proposed methodology is applicable to sand casting. However, there is a need to extend this framework to other casting processes like die casting and investment castings by adding suitable constraints that limits the process.

The proposed work assumes that location of ingate is fixed and so only requirement is to optimize the gating dimensions. However there is a need to add the ingate location constraint, so that layout of gating system along with gating dimensions both can be optimized.

References

1. Kannan S, “Computer simulation and water modeling of fluid flow in simple horizontal and vertical gating systems” Master Thesis, University of Wisconsin-Madison, 1991
2. Miller D.S, “A Guide to Losses in Pipe and Duct System”, British hydrodynamics Research Association, Cranfield, UK, 1971
3. Gardel A, “Pressure drops in flows through T-shaped pipe fittings”. Bull. Technology. de la Suisse Romande, Vol. 83 pp 143-148, 1957
4. Vanderplaats G.N, “Numerical Optimization Techniques for Engineering Design: With Applications”, McGraw-Hill, New York, 1984
5. Armour Research Foundation of Illinois Institute of Technology, “ Fluid Flow Mechanics of Molten Steel” Chicago, 1951
6. Carlos E. Esparza, Guerrero-Mata, Martha P, Roger Z, “Optimal design of gating system by gradient search methods” *journal of Computational Materials Science*, Vol. 36, pp.457–467, 2006
7. Ravi B, “Metal casting-computer aided design and analysis” *Department of Mechanical engineering IIT Bombay*, 2006
8. Ruddle R. W, “The Running and Gating of Sand Castings: a review of the literature”, Institute of Metals, Monograph No. 19, 1956
9. Benedict R. P, “Fundamentals of Pipe Flow” John Wiley and Sons, New York, 1980
10. Campbell J, “Castings”, Butterworth-Heinemann, London, 1991
11. Campbell J, “Casting practice: The ten rules of castings” Technology and Engineering , 2004
12. Bradley F, Heinemann S “A hydraulics-based optimization methodology for gating design”, *Applied Mathematical Modelling* Vol. 17, pp 406–414, 1993
13. McDavid R.M, Dantzig J.A, “Design sensitivity and finite element analysis of free surface flows with application to optimal design of casting rigging systems” *International Journal for Numerical Methods in Fluids* Vol. 28, pp.419-442, 1998
14. McDavid R.M, Dantzig J.A, “Experimental and numerical investigation of mold filling, in: Modeling of Casting”, *Welding and Advanced Solidification Processes (MCWASP VIII) Chicago*, pp 59–66, 1998

15. Jong W.R, Wang K.K, "Automatic and optimal design of runner systems in injection moulding based on the flow simulation", *SPE Annual Technical Conference*, pp 554–560, 1990
16. Lee B.H, Kim B.H, "Optimization of part wall thickness to reduce warpage of injection-mould parts based on the modified complex method", *Polymer-Plastics Technology and Engineering*, Vol. 34, pp 793–811, 1995
17. Balasubramanian S. and Norrie D. H, " A multi agent intelligent design system integrating manufacturing and shop floor control*", International Conference on Multi Agent Systems (San Francisco, CA, USA),* pp 3–9, 1995
18. Lange, E.A and Bukowaski A.T, "Pouring Time for Steel Casting", US Navel Research Laboratory, Washington, DC.1958
19. Iyengar S.N, "Gating and Risering systems". Indian Foundry J, pp 37-38, 2002
20. Ranjan R, Kumar N, Pandey R.K and Tiwari M.K, "Agent-based design framework for riser and gating system design for sound casting", *International Journal of Production Research*, vol. 42:22, pp 4827 – 4847, 2004
21. Pandelidis I, Zou Q, Lingard T, "Optimization of Gate Location and Operational Molding Conditions for Injection Molding", *Annual Technical Conference of the Society of Plastics Engineers (ANTEC), Atlanta, Georgia, USA*, pp 18–21,1988
22. Bose P, Toussaint G "Computing the Constrained Euclidean, Geodesic and Link Centre of a Simple Polygon with Applications" pp 102–111, 1996
23. Saxena M, Irani R.K, "Automated Gating Plan Synthesis for Injection Molds" *Computer Engineering ASME*, Vol. 1, pp 381-389, 1992
24. Ong S K, Pormbanpong S, Lee K.S, "An object-oriented approach to computer-aided design of a plastic injection mould" *Journal of Intelligent Manufacturing* Vol. 6, pp 1–10, 1995
25. Mehl DC, Belter KA, Ishil K, "Design for Injection Molding: Using Dimensional Analysis to Assess Fillability" *Advanced Design Automation* ,Vol 69, pp 427–434, 1994
26. Saxena M, Irani R. K, "An Integrated NMT-Based CAE Environment - Part I: Boundary-Based Feature Modeling Utility" *Engineering with Computers* Vol.9, pp 210–219, 1993
27. Lee B H, Kim B.H, "Automated Selection of Gate Location Based on Desired Quality of Injection Molded Part" *Annual Technical Conference of the Society of Plastics Engineers (ANTEC), Boston, USA*, pp 554-560, 7–11, 1995

28. Young W.B, " Gate Location Optimization in Liquid Composite Molding Using Genetic Algorithm" *journal of Composite Materials,* Vol. 28, pp 1098–1113, 1994
29. Lam Y. C, Seow L.W, "Cavity Balance for Plastic Injection Molding" *Polymer Engineering Science*, Vol. 40, pp 1273–1280, 2000
30. Lam Y.C, Jin S, "Optimization of Gate Location for Plastic Injection Molding" *Journal of Injection Molding Technology*, Vol.5, pp 180–192, 2001
31. Irani R.K, Saxena M, "An Integrated NMT-Based CAE Environment - Part II: Applications to Automated Gating Plan Synthesis for Injection Molding" *Engineering with Computers*, Vol. 9, pp 220–230,1993
32. Lam Y.C, Britton G.A, Liu D.S, "Optimization of gate location with design constraints", *International Journal of Advanced Manufacturing Technology*, Vol. 24, pp 560–566, 2004
33. Ravi B, Shrinivasan M.N, "Computer aided gating and metal rising simulation", 40th Indian Foundry Congress, Institute of Indian Foundry men, Madras, 1992
34. Sirrell B, Holliday M, Campbell J, "Benchmark testing the flow and solidification modeling of Al castings" *Journal of Materials*, Vol. 48, pp 20 - 23, 1996
35. Wukovich N, Metevelis G, "Gating :The Foundry man's Dilemma or Fifty Years of Data & still Asking How?" *AFS Transactions* , Vol. 97, pp 295, 1989
36. Sarkar Samir, "Fuels and combustion" *Department of chemical engineering IIT Bombay*, pp 41 – 44, 2008

Appendix I

Algorithm of the SQP process

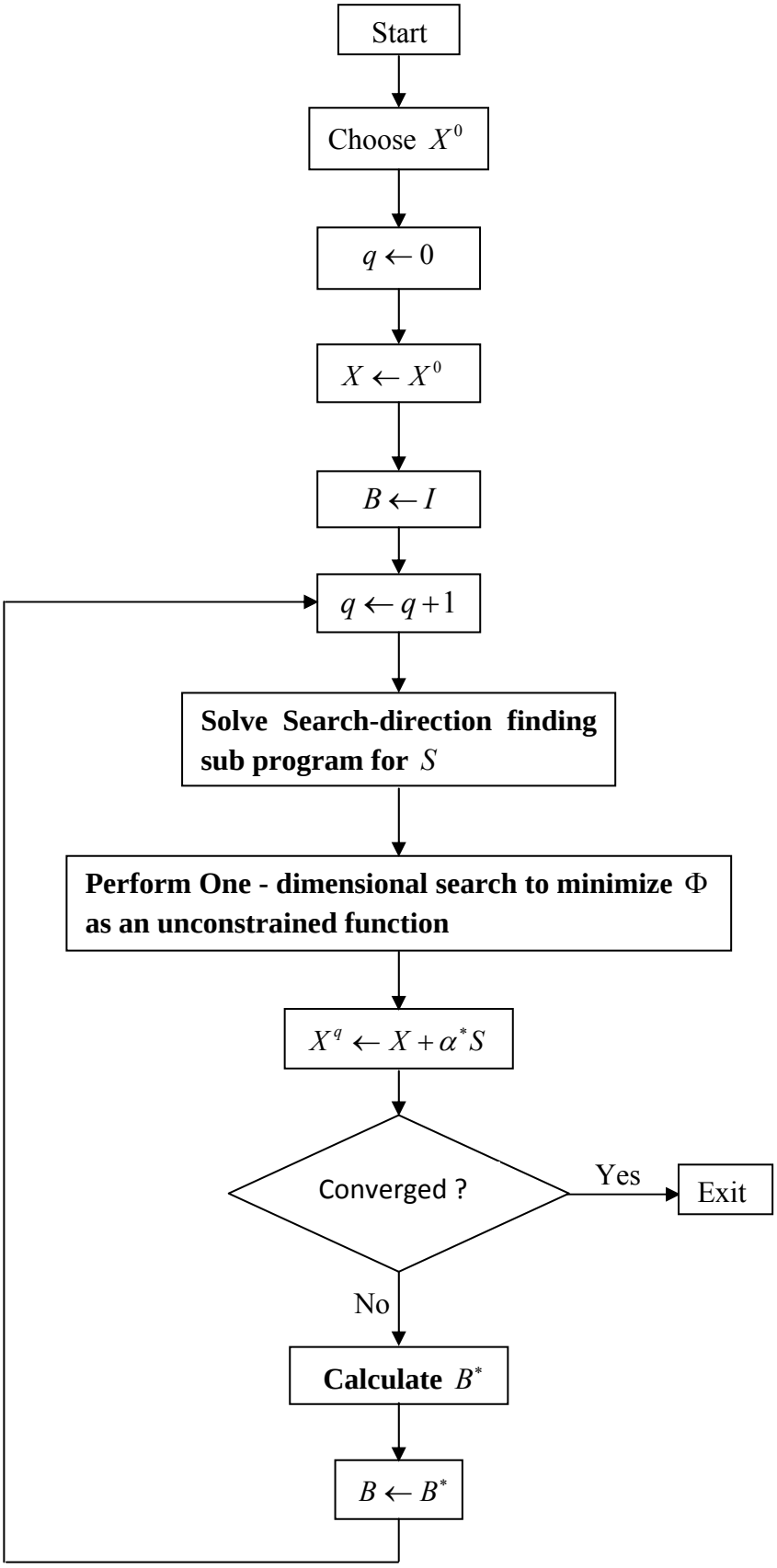

Algorithm to For Search Direction S

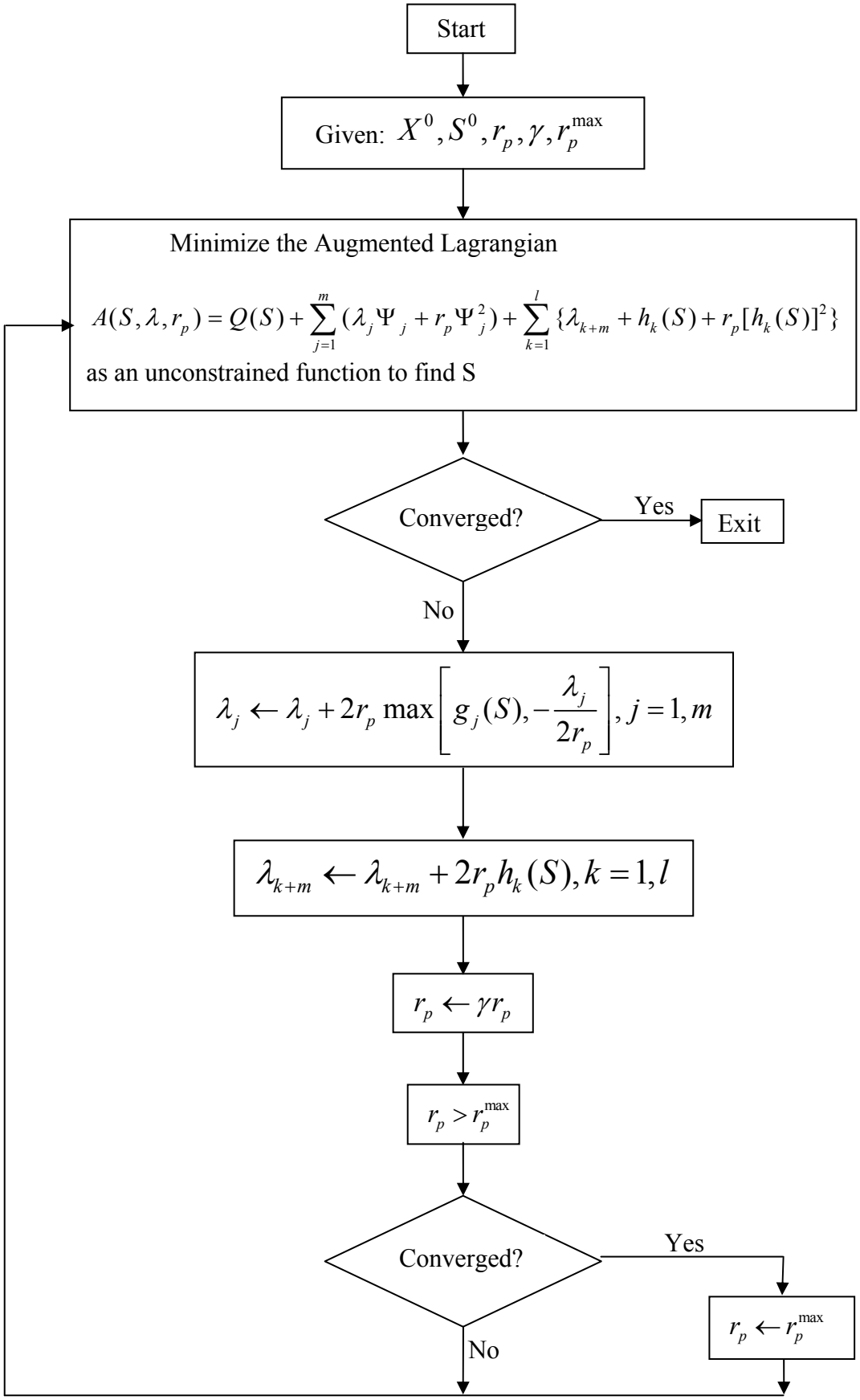

Algorithm for One dimensional Search to get α^*

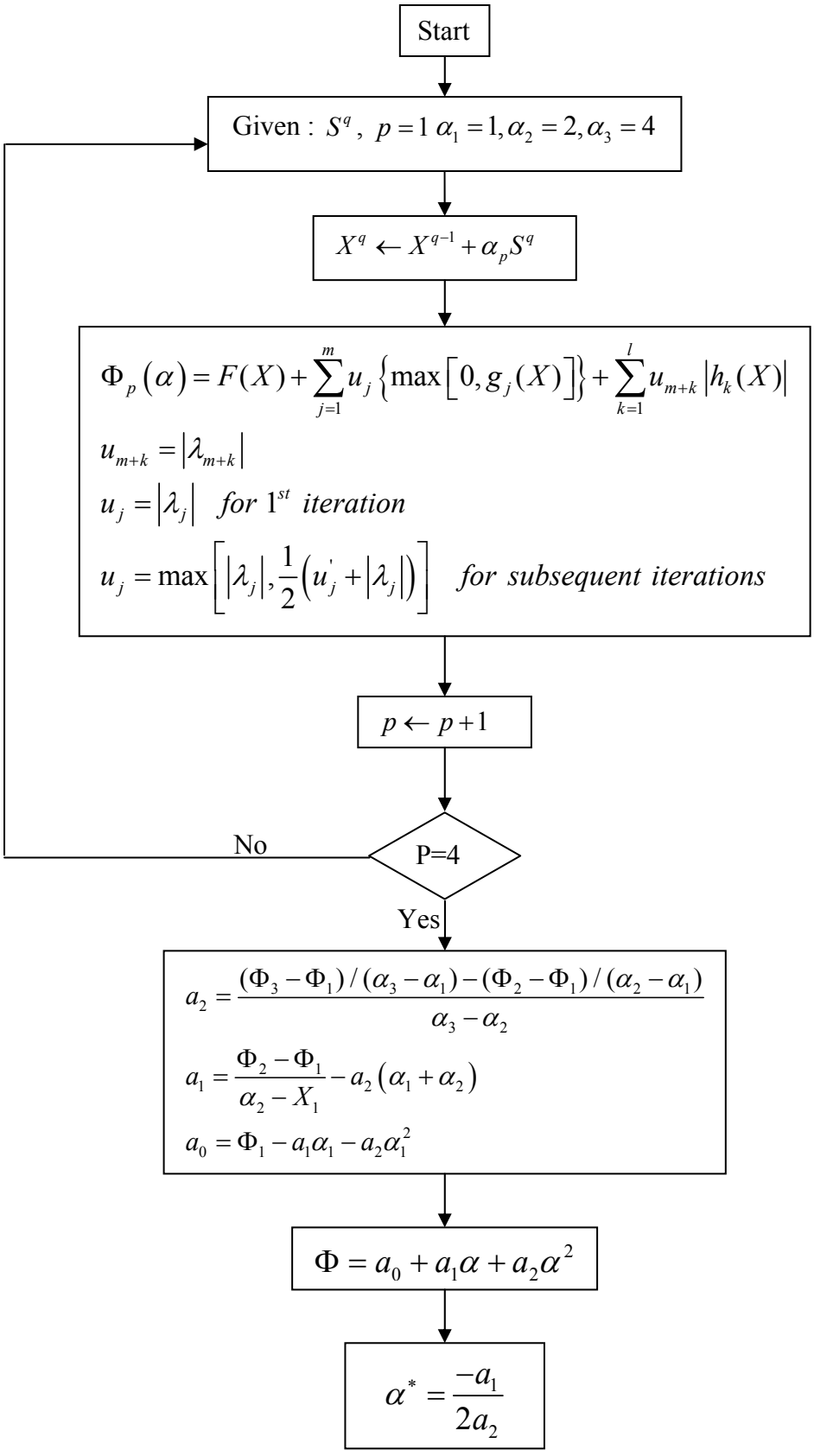

Appendix II

```
clear
clc
format long
syms x1 x2 f g s1 s2 alphaa fb fc phi
syms lamda1 lamda2 lamda3
% define objective function
iter = 0;
of = -2700*x1*x2;
% defining constraints
% taking Ag = x1 & Vg = x2

%*************formulation of constraint starts**********************

% casting dimensions
l_cast = 0.100;
b_cast = 0.200;
h_cast = 0.300;

tm                                  =                                   0.020;
%  mold thk

% mold dimensions
l_mold =l_cast+2*tm+0.060;
b_mold =b_cast+2*tm;
h_mold =h_cast+2*tm;

%Initial mold height
% input initial mold height ht = casting height + mold thk(1 inch min.)
% in our case ht = h+0.04 =0.1+0.04=0.140 mtr
ht = h_cast+tm;

Ai = l_cast*b_cast;
tau_f =15;
dl                                  =                                   0.005;
% layer thk.
rho = 2380;
rho_sand = 1600;
Sy                                  =                                  117198;
% mold compressive strength
meu = 0.012;
pour_ht = 0.03;
t_efft          =          0.002                                             ;
% effective thk.
rho_seacoal = 0.56*1e3;
M_Co2 = 43.991;
M_N2  = 28.01;
M_H2  = 2*1.0079;
M_O2  = 31.98;
M_H2O = 18;
Ti = 948;
rho_H2O = 1000;
R_H2O = 287;
p_air_0 = 101325;
f_per = 90;

% forulation of constraint 1(pouring time)
g(1) = sqrt(2/9.81)*Ai*(sqrt(ht)-sqrt(ht-h_cast))/tau_f - x1;
```

```
%formulation of constraint 2(modulus)
V_cast =l_cast*b_cast*h_cast ;
A_surf = 2*(l_cast*b_cast+b_cast*h_cast+h_cast*l_cast);
% cooling surface area of connected section
% for square ingate pg=sqrt(Ag)
g(2) = x1-16*(V_cast/A_surf)^2;
% formulation of constraint 3(mold erosion)

h_star = ht-tm-h_cast/2;

g(3)= x2-Sy/(rho*sqrt(2*9.81*h_star)) ;

% formulation of constraint 4  (Reynold No.)
g(4)=x2*sqrt(x1)-(meu/rho)*20000;

% formulation of constraint 5 (Quick filling)
m_box_vol = l_mold*b_mold*h_mold;
m_cavi_vol= V_cast;

sand_vol = m_box_vol - m_cavi_vol;
p_metal=2700*9.81*(ht+ pour_ht - dl);

V_layer_i=l_cast*b_cast*dl;
V_i=l_cast*b_cast*(h_cast-dl);
% gas volume
tau_i=V_layer_i/(x1*x2);
% time to fill dl
t_san_wt = rho_sand * sand_vol;
o_vol = (l_cast+2*t_efft)*(b_cast+2*t_efft)*(dl+t_efft);
% outer vol up to thk dl
sea_coal_vol = 0.05*(o_vol-V_layer_i);
sea_coal_wt=rho_seacoal*sea_coal_vol*1e3 ;
% in grams
c_per = 0.85*sea_coal_wt;
m_H2 = 0.01*sea_coal_wt;
m_N2 = 0.07*sea_coal_wt;
m_O2 = 0.07*sea_coal_wt ;

m_Co2= c_per*43.991/12.011 ;
% no. of mole fraction of gases
n_Co2= m_Co2/M_Co2;
n_H2= m_H2/M_H2;
n_N2= m_N2/M_N2;
n_O2= m_O2/M_O2;

% calculation of gas constant of the gases
R_Co2= 8.314/M_Co2;
R_H2 = 8.314/M_H2;
R_N2 = 8.314/M_N2;
R_O2 = 8.314/M_O2;

% calculating partial pressure of gases
p_Co2=n_Co2*R_Co2*Ti/V_i;
p_H2=n_H2*R_H2*Ti/V_i;
p_N2=n_N2*R_N2*Ti/V_i;
p_O2=n_O2*R_O2*Ti/V_i;

% moisture gases
```

```
V_H2O = 0.04*(o_vol-V_layer_i);
m_H2O = rho_H2O*V_H2O*1e3     ;                          % grams

m_H2_moist=m_H2O*(M_H2/M_H2O)*1e-3 ;
m_O2_moist=m_H2O*(16/M_H2O) ;

% no. of mole fraction of gases

n_H2_moist= m_H2_moist/M_H2;
n_O2_moist= m_O2_moist/M_O2;

% calculating partial pressure of gases
p_H2_moist=n_H2_moist*R_H2*Ti/V_i;

p_O2_moist=n_O2_moist*R_O2*Ti/V_i ;

% Increase in air pressure
V_0 =l_cast*b_cast*h_cast;
T_air = 948;
R_air = 287;
m_air_1=p_air_0*V_0/(R_air*T_air);
p_air_1=m_air_1*R_air*T_air/V_i;
p_gas_per=V_i*tm/(sand_vol*f_per*tau_i) ;
p_gas_i=(p_Co2+p_H2+p_N2+p_O2)+(p_H2_moist+p_O2_moist);
p_mold_i=p_gas_i+p_air_1-p_air_0-p_gas_per;
g(5) = p_mold_i-p_metal

%*************formulation of constraint ends*********************

x = [0.00009885 ; 2];
%evaluate the obj fun and constraints at the initial design vector
fX = subs(of,{x1,x2},{x(1),x(2)});
% fprintf('\nThe value of objfun at Design vector is fX : '),disp(fX)
g1X = subs(g(1),{x1,x2},{x(1),x(2)});
if g1X < 1e-3 && g1X > 0,
g1X = 0;
end
% fprintf('\nThe value of confun at Design vector is g1X : '),disp(g1X)
g2X = subs(g(2),{x1,x2},{x(1),x(2)});
if g2X < 1e-3 && g2X > 0,
g2X = 0;
end
% fprintf('\nThe value of confun at Design vector is g2X : '),disp(g2X)

g3X = subs(g(3),{x1,x2},{x(1),x(2)});
if g3X < 1e-3 && g3X > 0,
g3X = 0;
end
% fprintf('\nThe value of confun at Design vector is g3X : '),disp(g3X)

g4X = subs(g(4),{x1,x2},{x(1),x(2)});
if g4X < 1e-3 && g4X > 0,
g4X = 0;
end
% fprintf('\nThe value of confun at Design vector is g4X : '),disp(g4X)

g5X = subs(g(5),{x1,x2},{x(1),x(2)});
if g5X < 1e-3 && g5X > 0,
g5X = 0;
```

```
end
% fprintf('\nThe value of confun at Design vector is g5X : '),disp(g5X)


%objective function gradients
df1 = diff(of,x1);
df2 = diff(of,x2);

%costraint gradients
dg1x1 = diff(g(1),x1);
dg1x2 = diff(g(1),x2);

dg2x1 = diff(g(2),x1);
dg2x2 = diff(g(2),x2);

dg3x1 = diff(g(3),x1);
dg3x2 = diff(g(3),x2);

dg4x1 = diff(g(4),x1);
dg4x2 = diff(g(4),x2);

dg5x1 = diff(g(5),x1);
dg5x2 = diff(g(5),x2);


% value of the objective fuction gradient at the initial design vector
dfX = subs({df1,df2},{x1,x2},{x(1),x(2)});
% fprintf('\nThe gradient of objfun at Design vector is:  dfX '),disp(dfX)

% value of the constraint gradients at the initial design vector
dg1X = subs({dg1x1,dg1x2},{x1,x2},{x(1),x(2)});
% fprintf('\nThe gradient of g1     at Design vector is: dg1X '),disp(dg1X)
dg2X = subs({dg2x1,dg2x2},{x1,x2},{x(1),x(2)});
% fprintf('\nThe gradient of g2     at Design vector is: dg2X '),disp(dg2X)
dg3X = subs({dg3x1,dg3x2},{x1,x2},{x(1),x(2)});
% fprintf('\nThe gradient of g3     at Design vector is: dg3X '),disp(dg3X)
dg4X = subs({dg4x1,dg4x2},{x1,x2},{x(1),x(2)});
% fprintf('\nThe gradient of g4     at Design vector is: dg4X '),disp(dg4X)
dg5X = subs({dg5x1,dg5x2},{x1,x2},{x(1),x(2)});
% fprintf('\nThe gradient of g5     at Design vector is: dg5X '),disp(dg5X)


HS = eye(2);
% the new objective function can be given by
epsi2 =3;
while epsi2>=1e-3
iter = iter+1;
dfS = subs({df1,df2},{x1,x2},{s1,s2});
%  fprintf('\nThe  gradient  of  objfun  at  New  Design  vector  S  is:  dfS
'),disp(dfS)
S = [s1 ; s2];

Qs = dfS*S+0.5*S.'*HS*S
expand(Qs);
%   fprintf('\nThe   new   objfun   at   New   Design   vector   S   is:   QS
'),disp(expand(Qs))
if g1X < 0,
    beta1 = 1 ;
else
```

```
    beta1 = 0 ;
end
% fprintf('\nbeta1 = '),disp(beta1)

if g2X < 0,
    beta2 = 1;
else
    beta2 = 0;
end
% fprintf('\nbeta2 = '),disp(beta2)

if g3X < 0,
    beta3 = 1;
else
    beta3 = 0;
end

if g4X < 0,
    beta4 = 1;
else
    beta4 = 0;
end

if g5X < 0,
    beta5 =1;
else
    beta5 = 0;
end


gS(1) = beta1*g1X + dg1X*S;
fprintf('\nThe the new constraint at New Design vector S is g1S =
'),disp(gS(1))
gS(2) = beta2*g2X + dg2X*S;
fprintf('\nThe the new constraint at New Design vector S is g2S =
'),disp(gS(2))
gS(3) = beta3*g3X + dg3X*S;
fprintf('\nThe the new constraint at New Design vector S is g3S =
'),disp(gS(3))
gS(4) = beta4*g4X + dg4X*S;
fprintf('\nThe the new constraint at New Design vector S is g4S =
'),disp(gS(4))
gS(5) = beta5*g5X + dg5X*S;
fprintf('\nThe the new constraint at New Design vector S is g5S =
'),disp(gS(5))



hessian = [jacobian(jacobian(Qs))];
H = combine(hessian)


% ---------- calculation of f matrix starts -----------------------

 [p,t1]=coeffs(Qs,s1);
 [q,t2]=coeffs(Qs,s2);
 f =[]

if length(t1) == 3                                    %  [ s1^2,s1,1 ]
```

```
    k2 = findsym(p(2));
        if k2 == s2
        f(1,1) = subs(p(2),s2,0);
        else
            f(1,1)= p(2)  ;
        end
elseif length(t1) == 2 && t1(1)== s1                    %  [ s1,1 ]
    k2 = findsym(p(1));
        if k2 == s2
        f(1,1) = subs(p(1),s2,0);
        else
            f(1,1)= p(1);
        end
elseif length(t1) == 2 && t1(1)== s1^2 && t1(2)==1      %  [ s1^2,1 ]
        f(1,1) = 0;
elseif length(t1) == 2 && t1(1)== s1^2 && t1(2)==s1     %  [ s1^2,s1 ]
    k2  = findsym(p(2));
        if k2 == s2
            f(1,1) = subs(p(2),s2,0);
        else
            f(1,1) = 0 ;
        end
elseif length(t1) == 1 && t1(1) == 1                    %  [ 1 ]
     f(1,1) = 0;
elseif length(t1) == 1 && t1(1)==  s1                   %  [ s1 ]
     f(1,1) = p(1);
elseif length(t1) == 1 && t1(1)== s1^2                  %  [ s1^2 ]
      f(1,1) = 0;
end

if length(t2) == 3                                      %  [ s2^2,s2,1 ]
    k2 = findsym(q(2));
        if k2 == s1
        f(2,1) = subs(q(2),s1,0);
        else
            f(2,1)= q(2);
        end
elseif length(t2) == 2 && t2(1)== s2                    %  [ s2,1 ]
    k2 = findsym(q(1))
        if k2 == s1
        f(2,1) = subs(q(1),s1,0);
        else
        f(2,1)= q(1);
        end
elseif length(t2) == 2 && t2(1)== s2^2 && t2(2)==1      %  [ s2^2,1 ]
        f(2,1) = 0;
elseif length(t2) == 2 && t2(1)== s2^2 && t2(2)==s2     %  [ s2^2,s2 ]
    k2  = findsym(q(2));
        if k2 == s1
            f(2,1) = subs(q(2),s1,0);
        else
            f(2,1) = 0 ;
        end
elseif length(t2) == 1 && t2(1) == 1                    %  [ 1 ]
     f(2,1) = 0;
elseif length(t2) == 1 && t2(1)==  s2                   %  [ s2 ]
     f(2,1) = q(1);
elseif length(t2) == 1 && t2(1)== s2^2                  %  [ s2^2 ]
      f(2,1) = 0 ;
end
```

```
% ---------- calculation of f matrix ends ----------------------

%*********************************************************************%

%************calculation of A and b matrix starts*******************%

A = [];b=[];
for ii =1:5
[w1 c1] = coeffs(gS(ii),s1);
[w2 c2] = coeffs(gS(ii),s2);

if length(c1)==2
  A(ii,1) = w1(1);
   k1 = findsym(w1(2));
   if k1 == s2
      b(ii,1) = (-1)*subs(w1(2),s2,0);
   else
     b(ii,1) = (-1)*w1(2)  ;
   end

elseif length(c1)==1 && c1(1) == s1
  A(ii,1) = w1(1);
  b(ii,1) = 0;

elseif length(c1)==1 && c1(1) == 1
  A(ii,1) = 0   ;
  k1 = findsym(w1(1));
    if k1 == s2
      b(ii,1) = (-1)*subs(w1(1),s2,0) ;
    else
     b(ii,1) = (-1)*w1(1)  ;
    end
end

if length(c2)==2
  A(ii,2) = w2(1);
elseif length(c2)==1 && c2(1) == s2
  A(ii,2) = w2(1);
elseif length(c2)==1 && c2(1) == 1
  A(ii,2) = 0;
end
end
 disp(A)
 disp(b)

%************calculation of A and b matrix ends*******************%

[s,fval,exitflag,output,lambda] = quadprog(H,f,A,b,[],[])
S = [s(1); s(2)]
%new design vector X is given by
X1 = alphaa*S + x

phi                                                                 =
subs(of,{x1,x2},{X1(1),X1(2)})+lambda.ineqlin(1)*subs(g(1),{x1,x2},{X1(1),X
1(2)})+                  lambda.ineqlin(2)*subs(g(2),{x1,x2},{X1(1),X1(2)})+
lambda.ineqlin(3)*subs(g(3),{x1,x2},{X1(1),X1(2)})+lambda.ineqlin(4)*subs(g
(4),{x1,x2},{X1(1),X1(2)})+lambda.ineqlin(5)*subs(g(5),{x1,x2},{X1(1),X1(2)
})
```

```
if lambda.ineqlin(1)== 0 && lambda.ineqlin(2)== 0 && lambda.ineqlin(3)==0
&& lambda.ineqlin(4)==0 && lambda.ineqlin(5)==0
    error('phi became linear so cannot solve the problem, for solving enter
another initial design vector')
end

%******quadratic interpolation technique start*********************%
syms alphaa
%Input the function phi
fa = subs(phi,alphaa,0)
t0 = 0.5
f1 = subs(phi,alphaa ,t0)


while f1< fa
 fb  = f1
 f2 = subs(phi,alphaa,2*t0)
            if f2 > f1
               fc = f2
               break;
            else
                f1 = f2;
                t0 = 2*t0  ;
            end
end

if f1>fa
fc = f1 ;
fb = subs(phi,alphaa,t0/2);
end
a1 = fa;
b1 = (4*fb-3*fa-fc)/(2*t0);
c1 = (fc+fa-2*fb)/(2*t0^2);
alpha_bar  = -b1/(2*c1);
if  alpha_bar==Inf;
 alpha_bar= 10;
end

h = a1+b1*alpha_bar + c1*alpha_bar^2;
fbar= subs(phi,alphaa,alpha_bar );
% convergence criteria
%--------------------------------
 epsilonn = abs((h-fbar)/fbar)
 epsilonn =1000;
%--------------------------------
 A1 = 0;
 B1 = t0;
 C1 = 2*t0;

while epsilonn > 1e-03
    if alpha_bar >B1 && fbar<fb
        A1 = B1
        B1 = alpha_bar
        C1 = C1
    elseif alpha_bar >B1 && fbar>fb
        A1 = A1
        B1 = B1
        C1 = alpha_bar
    elseif alpha_bar <B1 && fbar<fb
        A1 = A1
```

```
        C1 = B1
        B1 = alpha_bar
    elseif alpha_bar <B1 && fbar>fb
        A1 = alpha_bar
        B1 = B1
        C1 = C1
    end
    fa = subs(phi,alphaa,A1);
    fb = subs(phi,alphaa,B1)
    fc = subs(phi,alphaa,C1);
 a1   =   (fa*B1*C1*(C1-B1)+fb*C1*A1*(A1-C1)+fc*B1*A1*(B1-A1))/((A1-B1)*(B1-
C1)*(C1-A1));
 b1  =  (fa*(B1^2-C1^2)+fb*(C1^2-A1^2)+fc*(A1^2-B1^2))/((A1-B1)*(B1-C1)*(C1-
A1));
 c1= -(fa*(B1-C1)+fb*(C1-A1)+fc*(A1-B1))/((A1-B1)*(B1-C1)*(C1-A1));
 alpha_bar    =  (fa*(B1^2-C1^2)+fb*(C1^2-A1^2)+fc*(A1^2-B1^2))/(2*(fa*(B1-
C1)+fb*(C1-A1)+fc*(A1-B1)))
 if  alpha_bar==Inf;
    break;
end
alpha_opt = alpha_bar
 h = a1+b1*alpha_bar +c1*alpha_bar^2;
 fbar= subs(phi,alphaa ,alpha_bar )
 epsilonn = abs((h-fbar)/fbar);
end
if  alpha_bar==Inf;
    alpha_bar= 10;
    alpha_opt = alpha_bar
elseif alpha_bar==NaN
    alpha_bar= 20;
    alpha_opt = alpha_bar
    alpha_opt = alpha_bar
end

%******quadratic interpolation technique end **********************%
if iter ==1
X2old = x ;
else
X2old = X2;
end
X2 = alpha_opt*S + X2old;
X2new = X2
if X2new(1)<0 || X2new(2)<0
  X2new = X2old
    break;
end
P = X2new- X2old;
fXold = subs(of,{x1,x2},{X2old(1),X2old(2)});
fX = subs(of,{x1,x2},{X2new(1),X2new(2)});
fprintf('\nThe value of objfun at Design vector is fX : '),disp(fX)
L    =        of    +    lambda.ineqlin(1)*g(1)+    lambda.ineqlin(2)*g(2)+
lambda.ineqlin(3)*g(3)+ lambda.ineqlin(4)*g(4)+ lambda.ineqlin(5)*g(5);
dLx1 = diff(L,x1);
dLx2 = diff(L,x2);

dLX2 = subs({dLx1;dLx2},{x1,x2},{X2new(1),X2new(2)});
dLX1 = subs({dLx1;dLx2},{x1,x2},{X2old(1),X2old(2)});

Q = dLX2 - dLX1;
z1 =0.2*P'*HS*P;
z2 =P'*Q;
```

```
if z2<z1
    theta = (4*z1/(5*z1-z2));
else
    theta = 1.00;
end

gamma   = theta*Q +(1-theta)*HS*P;
% = [0.54914;-0.32518];
HS = HS -((HS*P*P'*HS)/(P'*HS*P))+ ((gamma*gamma')/(P'*P));
epsi2 = abs(fX-fXold)
end
```

Acknowledgement

It gives me an immense pleasure and gratitude to extend my sincere thanks to my guide **Prof. B. Ravi,** Mechanical Engineering Department for his consistent, invaluable co-operation and guidance during the course of my project work. The days spent with him form the best period of my professional training and satisfying achievement. I remember with great emotion, the guidance, generous support that went beyond academics.

The salient support, best wishes and blessings of my parents and family have been the constant source of inspiration and encouragement for me. Finally I am very much thankful to my colleagues for their co-operation and support.

Vaghasia Dolar Kanjibhai
IIT Bombay, Powai
June, 2009